American Mineralogist, Volume 69, pages 601–621, 1984

An orbital interpretation of Pauling's rules

JEREMY K. BURDETT[1] AND TIMOTHY J. MCLARNAN

Department of Chemistry
The University of Chicago, Chicago, Illinois 60637

Abstract

Pauling's rules, first collected together over fifty years ago, have traditionally been associated with electrostatic, "ionic" ideas of bonding in solids. In this paper we use a purely orbital model to tackle some of the structural predictions made by the rules. As a result of band structure computations on several model structures we present a scheme which focuses attention on the local anion coordination. We also use simple orbital based perturbation theoretical ideas to present a unifying explanation for Pauling's electrostatic bond strength sum rule and for the first time one for Baur's extension of it. In almost all areas the predictions of the rules and those of the covalent approach are similar, but their explanations are very different. The ideas presented lead to a new level of understanding concerning the structures of solids. These ideas have close ties with current models of molecular stereochemistry.

Introduction

In 1929, Pauling proposed a collection of five rules governing the geometries of ionic crystals (Pauling, 1929). These rules and the body of additions and emendations surrounding them passed rapidly into the accepted folklore of crystal chemistry, and for more than 50 years they have remained important and largely successful guides for mineralogists and solid state structural chemists.

In their original formulation, Pauling's rules were presented primarily as *ad hoc* generalizations useful in developing the hypothetical geometric models which were necessary to the solution of complex crystal structures using the experimental methods available in the 1920's. While several of the rules are given interpretations based on the ionic model, their proof is clearly in their applicability to real structures rather than in the details of somewhat vague ionic arguments. Further, nonionic ways of looking at crystals enter implicitly even in 1929 (see Pauling's remark that 6-membered rings occur in beryl because the bond angle at the oxygen atom in such rings approximates the tetrahedral angle). In his later writings Pauling (1960) is quite explicit in claiming that even quite covalent materials may obey rules isomorphous to some of those applying in ionic crystals. Despite efforts to distinguish between geometric precepts and a particular method of computing crystal energies, Pauling's rules have frequently been identified with the ionic model, and the success of those rules has often been used as an argument for the ionic nature of the bonding in such compounds.

Since about 1970, Gibbs and Tossell and their coworkers (Gibbs et al., 1981; Tossell and Gibbs, 1978) have made substantial progress in clarifying the origins of Pauling's rules by showing that many of his geometric predictions, most notably the shortening of shared polyhedral edges, are consequences not only of ionic arguments but also of more or less covalent effects which can be studied by performing molecular orbital calculations. At present the results of such computations have led to predictions of bond angles, the variations of bond strengths with bond angles, and so on, which in general seem in very good agreement with observation. Unfortunately, the methods of Tossell and Gibbs have required them to perform calculations not on crystals as a whole but on "molecular" fragments chosen to mimic local regions within a crystal. This is usually not a limitation in investigating *local* geometric preferences, but it does mean that the energies of crystal structures which differ in basic atomic topology and connectivity cannot be compared. The most obvious way to discuss theoretically the electrostatic valence rule or the rules involving the destabilizing character of shared polyhedral elements is to compare the energies of real and hypothetical structures some of which obey and some of which disobey these rules. Calculations on small molecular clusters will not lead to such information.

In this paper, we present an interpretation of Pauling's rules based on the results of band structure calculations using the "tight binding" approximation. These are just covalent "molecular orbital" calculations applied not to such clusters but to the crystal as a whole. Using these

---

[1] Fellow of the Alfred P. Sloan Foundation and Camille and Henry Dreyfus Teacher-Scholar.

0003–004X/84/0708–0601$02.00

results we will obtain an electronic understanding of these rules compatible with the arguments presently used to rationalize a large number of *molecular* structures. This understanding has a simple geometric content based on the hybridization and coordination geometry of the *anions* in the crystal. The structures we will consider can be ordered energetically by considering anion coordination spheres. While our calculations and interpretation generally support Pauling's rules, we mention several interesting points at which our predictions differ from his.

The structure types we shall discuss are largely either wurtzite derivatives or dipolar tetrahedral structures (McLarnan and Baur, 1982). This choice is motivated by the desire to consider a large family of closely related types which are typical of mineral structures with 4-coordinated anions. We expect our major conclusions to apply to a far larger class of structures than those actually studied. Similarly, most of our calculations use atomic parameters for Be and O, not because of the overwhelming mineralogical importance of bromellite (wurtzite-type BeO), but because Be and O lie near the top of the periodic table and BeO seems a typical "ionic" wurtzite-type compound. None of our conclusions depend on this precise choice of parameters. In the final section we mention some structures with two- and three-coordinate anions.

In discussing our calculations, we shall often use the words "anion" and "cation" as a familiar shorthand for electronegative and electropositive atoms, respectively. This terminology is used solely for linguistic convenience, and is not intended to have any implication regarding the physical nature of the bonding in any compound.

Pauling's First Rule: ionic radii

"A coordinated polyhedron of anions is formed about each cation, the cation–anion distance being determined by the radius sum and the coordination number of the cation by the radius ratio." (Pauling, 1929). This is perhaps the best known of Pauling's rules and introduces the concept of atomic (or rather ionic) size. Because approximate molecular orbital methods predict bond distances poorly, we cannot directly use our band calculations to cast light on this rule. However we do wish to point out the progress made in recent years using Phillips' Mendeleyevian philosophy in the area of structural mapping (St. John and Bloch, 1974; Zunger and Cohen, 1978; Bloch and Schatteman, 1981; Burdett et al., 1982). An important result obtained by the use of pseudopotential radii (r_l) has been the much closer definition of atomic "size". More specifically the identification of r_l^{-1} with an electronegativity has allowed a close correspondence to be made between billiard-ball theories based on sphere packings and modern electronic ideas based upon orbital concepts. In this paper we will focus on the remaining Pauling rules.

Rule 2: electrostatic valence sums

"In a stable coordination structure the electric charge of each ion tends to compensate the strength of the electrostatic valence bonds reaching to it from the cations at the centers of the polyhedra of which it forms a corner; that is, for each anion

$$\zeta = \sum_i \frac{z_i}{\nu_i} = \sum_i s_i\text{''} \tag{1}$$

(Pauling, 1929). Here $-\zeta$ is the charge of an anion, i runs over all cations coordinated to that anion, z_i and ν_i are the charge and coordination numbers, respectively, of cation i, and $s_i = z_i/\nu_i$. This electrostatic valence rule, while only approximately satisfied by some compounds, has proven an enormous aid to mineralogists and crystallographers. It is, for example, the primary method for distinguishing O^{2-} from $(OH)^-$ and H_2O in complex mineral structures. Further, it was regarded by Bragg (1930) as the most important and innovative of Pauling's rules.

Pauling himself justified this rule by saying that configurations satisfying it placed highly charged anions at sites of large positive potential, and hence of high bond strength sums; though this argument does little to prove the equality of charge and bond sum. On the other hand, the validity of the rule for simple crystals follows from purely topological considerations: any binary compound in which all atoms of each type have the same coordination number must satisfy the rule.

Since formal charge is not a quantity appearing in the molecular orbital formalism, (although, given the molecular wavefunction we can calculate an atomic charge from a population analysis) it does not seem possible to use these calculations to test the valence sum rule numerically (i.e., to predict the allowable departure of Σs_i from ζ). It is possible, however, to ask whether such calculations predict qualitatively that more highly charged anions should occupy sites with larger bond sums. To do this we must consider a structure with more than one type of anion and with two or more cation species differing either in charge or coordination number or both. The only known such structure which is a derivative of the wurtzite type is that adopted by α-LiSiON (Laurent et al., 1980; Laurent et al., 1981; O'Keeffe et al., 1981), and probably by MgAlON and ZnAlON. This structure, shown in Figure 1, has a (2,1) unit cell; that is, it has $a = 2a_0$, $b = b_0$ and $c = c_0$, where a_0, b_0, c_0 are the axes of the smallest orthohexagonal cell of a hexagonal close packing. Also shown in Figure 1 are three other hypothetical structures representing the only ways to order equal numbers of two cations over the metal sites in the (1,1) wurtzite supercell. The notation employed for these types is that of McLarnan and Baur (McLarnan and Baur, 1982; Baur and McLarnan, 1982) who refer to α-LiSiON as the W-*Pbc*2_1 (2,1) type.

None of these four structure types exactly satisfies the

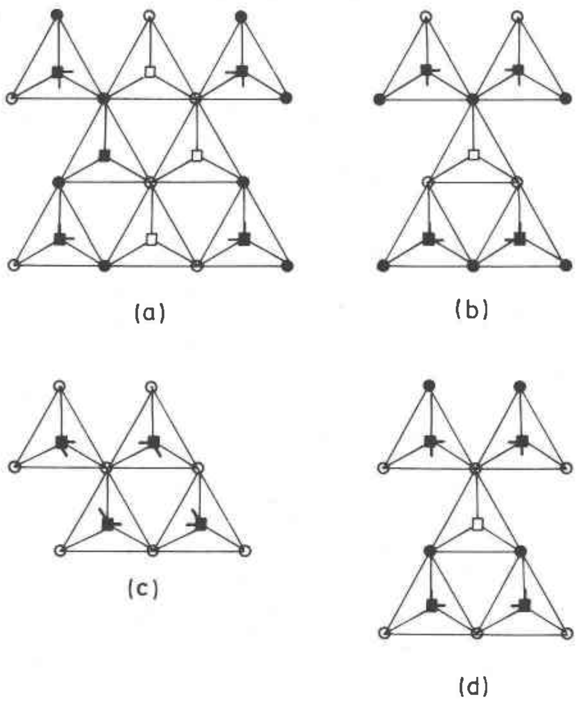

Fig. 1. Idealized crystal structures of α-LiSiON = W-$Pbc2_1$ (2,1) (a) and three hypothetical arrangements of the same stoichiometry: W-$Pmn2_1$ (1,1) (b), W-$P3m$ (1,1) (c) and W-$Pmc2_1$ (1,1) (d). The anions are hexagonally close packed and the cations fill tetrahedral holes. Filled squares = Si(0),N($\frac{3}{8}$); empty squares = Li(0),O($\frac{3}{8}$); filled circles = Si ($\frac{1}{2}$),N($\frac{7}{8}$); empty circles = Li($\frac{1}{2}$),O($\frac{7}{8}$). Only the cation tetrahedra at z = 0 are drawn. Structures b–d and their antistructures are the only ones geometrically possible for LiSiON with a (1,1) orthohexagonal cell.

electrostatic valence rule (Fig. 2). In three of them, α-LiSiON, W-$Pmn2_1$ (1,1) and W-$P3m$ (1,1), half of the anions are coordinated to 3 atoms of metal A and one of metal B, and the other half are coordinated to 3B + 1A. For (A,B) = (Li,Si) this produces bond strength sums of 3.25 and 1.75, while for (Mg,Al) the bond strength sums are 2.75 and 2.25. While the bond strength sums are not equal to 3 and 2, it is easy to see that they come as close to these values as is possible for wurtzite derivatives where all metal atoms of each kind are crystallographically equivalent. In the W-$Pmc2_1$ (1,1) type, every anion is coordinated by 2A + 2B, and hence has $\Sigma s_i = 2.5$.

We would like to show that in an ABON crystal with the W-$Pbc2_1$ (2,1), W-$Pmn2_1$ (1,1) or W-$P3m$ (1,1) structure, the nitrogen atoms will occupy the sites of higher bond sum, and that these structures all lie lower in energy than the W-$Pmc2_1$ (1,1) type in which O and N atoms see the same bond sum. The standard way of predicting site preferences of this sort using modern electronic ideas is to calculate the orbital wavefunction of a material in which O and N atoms are both replaced by hypothetical atoms intermediate in size and electronegativity, and then to determine the charge on each atom in this model crystal via a population analysis (Burdett, 1980; Chen and Hoffmann, 1976). In the real compound, the more electronegative O atoms can be expected to occupy the sites with the larger electron density (i.e., larger negative charge). In order to avoid confusing effects due to metal charge with those due to metal size, we have carried out such calculations for MgAlON rather than for LiSiON, and have further chosen identical Slater exponents for the two metals. Correspondingly, all calculations have been performed with equal cation–anion distances. The resulting charges are given in Table 1, which shows that indeed sites with small bond strength sums, which according to the second rule should be occupied by O rather than N, are significantly more electron rich. A further test of this is given in Table 2, which shows the site charges and energies of all four of these structures calculated not with averaged anions but with real O and N atoms. Values are shown for both the ordering expected from Pauling's rule and the opposite one. The correctly ordered structures lie lowest in energy, followed by those in which O and N occupy sites with equal electrostatic bond strength sum, followed by those in which N occupies sites with lower bond sum than O. Further, in the structures with the Pauling's rule-predicted ordering, there has been a migration of charge away from both N and Mg, the more electropositive anion and cation, toward both Al and O, the more electronegative pair.

The valence sum rule, however, says more than just that very electronegative cations, i.e., those with small negative formal charges, should be located in sites of small electrostatic valence sums. It also says that the bond strength sum should equal the negative of the formal charge. In our covalent language, this means that anions of the same electronegativity should be found in sites of equal bond sum. Thus, in calculations in which all anions are taken to be identical, the W-$Pmc2_1$ (1,1) structure in which every anion receives the same bond strength sum should be favored over the W-$P3m$ (1,1), W-$Pmn2_1$ (1,1)

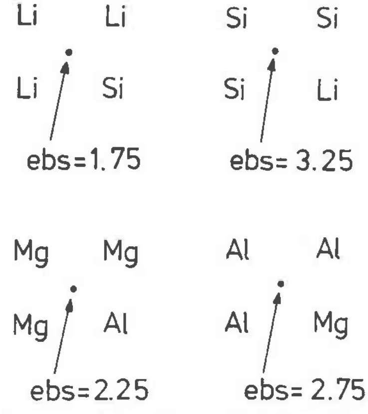

Fig. 2. Electrostatic bond sums for LiSiON and MgAlON in the structure types W-$Pmn2_1$ (1,1) or W-$P3m$ (1,1).

Table 1. Electronic charges in $MgAl(O,N)_2$ structures[a]

Σs_i	Structure	q
2.75	W-$Pbc2_1$(2,1)	7.5238
2.75	W-$Pmn2_1$(1,1)	7.5223
2.75	W-P3m(1,1)	7.5213
2.5	W-$Pmc2_1$(1,1)	7.5919
2.5	W-$Pmc2_1$(1,1)	7.5932
2.25	W-$Pbc2_1$(2,1)	7.6643
2.25	W-$Pmn2_1$(1,1)	7.6653
2.25	W-P3m(1,1)	7.6653

[a] The number, q, of valence electrons on sites with different electrostatic bond strength sums in $MgAl(O,N)_2$. Four different structures with this composition are considered. In these calculations all anions were given identical parameters intermediate between those of O and N, so that variations in q reflect differences associated with the sites, not with the nature of the anions. In this and other tables in the text we have deliberately reported more significant figures than perhaps absolutely necessary.

and W-*Pbc*2 (2,1) types in which half the anions have $\Sigma s_i = 2.25$, and half have $\Sigma s_i = 2.75$. That this is so is shown in Table 3, which gives the energies of these four structures with all the anions given equal parameters midway between those of O and N. We shall return below both to this calculated preference of identical anions for similar environments and to the significant fact that the energy differences in Table 3 are smaller than those in Table 2.

One other important variation on Pauling's second rule is the Zachariasen–Baur extension of it (Baur, 1970) to state that oversaturated anions should form unusually long bonds to their cation neighbors, and that undersaturated anions should form unusually short bonds. As shown by Baur (1981a) nearly all of the variation of individual Si–O bond lengths which can be attributed to any local effect is due to this relation between p_O, the electrostatic bond strength sum at an oxygen atom in the structure, and d(Si–O). Figure 3 plots the bond overlap populations of all crystallographically distinct Mg–O, Al–O, Mg–N and Al–N bonds in the eight structure types of Table 2 as a function of the electrostatic bond strength sum at the anion. These bond overlap populations are a measure of the calculated bond strength between two atoms, and hence normally correlate inversely with bond lengths. Thus, the calculated decreases in the bond overlap populations of all four types of bonds with increasing anion saturation represents a prediction by "molecular orbital" methods of exactly the qualitative bond length variations observed generally by Baur. We emphasize that these numbers come from computations which generate the band structure of the infinite crystal and not from molecular fragments. It is also important to note that all of the calculations are performed on structures with identical anion–cation distances so that there is no geometrical bias initially built into the problem. The effects we are seeing are purely electronic ones.

All of these results can be understood using the methods of perturbation theory (Burdett, 1980; Hoffmann, 1971) using well-known techniques. The occupied orbitals in MgAlON are largely located on the anions, so to evaluate the bonding energy of a particular structure for MgAlON we must ask how the anion levels are perturbed in the crystal from their energies in a free atom. These perturbations will arise on our model primarily from the strongest orbital interactions experienced by the anions, namely those with the neighboring metal atoms. Consider therefore the interaction of a single anion orbital with energy H_{11} with a single cation orbital with energy $H_{22} > H_{11}$ as in Figure 4. The magnitude of the interaction between these two orbitals is measured by their overlap integral S_{12}. It is therefore reasonable to write (Burdett, 1980) the energy of the perturbed anion orbital as a power

Table 2. Bond sums, charges and energies of MgAlON variants[a]

Structure	Σs_i(vu) O	Σs_i(vu) N	q(e^-) O	q(e^-) N	q(e^-) Al	q(e^-) Mg	Energy(eV)
W-$Pbc2_1$(2,1)	2.25	2.75	7.7647	7.3654	0.8255	0.0444	-291.212
W-$Pmn2_1$(1,1)	2.25	2.75	7.7659	7.3627	0.8209	0.0505	-291.212
W-P3m(1,1)	2.25	2.75	7.7673	7.3586	0.8271	0.0470	-291.224
W-$Pmc2_1$(1,1)	2.5	2.5	7.7127	7.4349	0.8269	0.0255	-291.153
W-$Pmc2_1$(1,1)*	2.5	2.5	7.7116	7.4383	0.8231	0.0270	-291.143
W-$Pbc2_1$(2,1)*	2.75	2.25	7.6508	7.5302	0.6813	0.1377	-290.742
W-$Pmn2_1$(1,1)*	2,75	2.25	7.6502	7.5310	0.6734	0.1453	-290.733
W-P3m(1,1)*	2.75	2.25	7.6510	7.5289	0.6787	0.1414	-290.743

[a] Eight possible structures for MgAlON, the bond sums at the anion sites, the number of valence electrons associated with each atom, and the calculated energy per formula unit. Structures marked with an asterisk have the same cation arrangement as their unstarred counterparts but have the positions of O and N reversed. The top three structures have the anion ordering expected from Pauling's second rule, the middle two have all anions in sites with the same bond sum, and the bottom three have an ordering opposite that expected. MgAlON is believed to be isostructural with α-LiSiON, which has the W-$Pbc2_1$(2,1) structure.

Table 3. Energies of some averaged MgAlON structures[a]

Structure	Energy(eV/fmla.unit)
W-$Pmc2_1$(1,1)	-290.938
W-P3m(1,1)	-290.802
W-$Pmn2_1$(1,1)	-290.796
W-$Pbc2_1$(2,1)	-290.801

[a] The energies of 4 possible structures for MgAlON, computed with both O and N replaced by an averaged anion with atomic parameters midway between theirs. The most stable structure type in this calculation, W-$Pmc2_1$(1,1) is the one in which all anions see equal bond strength sums of 2.5.

series in S_{12}. As long as H_{11},H_{22} and H_{22}–H_{11} are of the same order of magnitude, the leading terms in this series are $E_\ell = H_{11} + H_{22}^2S_{12}^2/(H_{11} - H_{22})$. Thus $\epsilon_{stab} = H_{22}^2S_{12}^2/(H_{11} - H_{22}) < 0$ is the first order energetic stabilization of the filled anion orbital. Often the numerator of this expression is sufficiently constant so that one can write $\epsilon_{stab}\ \alpha(H_{11} - H_{22})^{-1}$. Thus, the stabilization resulting from two interacting orbitals is inversely proportional to their energy difference. Further, these second order energy terms are additive so that if the anion is coordinated by several cations of energies H_{22}, H'_{22}, H''_{22}, . . . one has $\epsilon_{stab}\ \alpha(H_{11} - H_{22})^{-1} + (H_{11} - H'_{22})^{-1} + (H_{11} - H''_{22})^{-1} + \ldots$. The metal orbital is pushed up in energy, i.e., it is destabilized. Since it is unoccupied it will not contribute energetically to the problem and we will mention it no further.

The atomic orbitals in MgAlON increase in energy in the order O < N < Al < Mg. In structures ordered according to Pauling's second rule, the most numerous nearest neighbor interactions are between O and Mg and between N and Al. The common pairs of neighbors in structures with the opposite ordering are O–Al and N–Mg. Let H_i be the energy of an atom of element i. Then the effect of interchanging the anions (Fig. 2) in a structure satisfying Pauling's postulate is to replace contributions to the crystal binding energy proportional to $(H_O - H_{Mg})^{-1} + (H_N - H_{Al})^{-1}$ with terms proportional to $(H_O - H_{Al})^{-1} + (H_N - H_{Mg})^{-1}$. To determine whether or not this change is stabilizing, we evaluate $\Delta\epsilon_{stab} = (H_O - H_{Al})^{-1} + (H_N - H_{Mg})^{-1} - (H_O - H_{Mg})^{-1} - (H_N - H_{Al})^{-1} = [(H_O - H_{Al})^{-1} - (H_O - H_{Mg})^{-1}] + [(H_N - H_{Mg})^{-1} - (H_N - {-}_{Al})^{-1}]$. Expanding this yields $(H_{Al} - H_{Mg})\{[(H_O - H_{Al})(H_O - H_{Mg})]^{-1} - [(H_N - H_{Al})(H_N - H_{Mg})]^{-1}\}$. Since $H_O - H_{Al} < H_N - H_{Al}$ and $H_O - H_{Mg} < H_N - H_{Mg}$ and all four of these terms are negative, the expression in braces is negative and $\Delta\epsilon_{stab} > 0$. Thus the arrangement with the ordering predicted by Pauling's rule should be the more stable one, as observed and as calculated.

More generally, the consequence of this reasoning is that stable crystal structures should allow as many interactions as possible between electronegative cations and electropositive anions and between electropositive cations and electronegative anions. This conclusion is essentially equivalent to that arising in a slightly different context from Pearson's ideas of hard and soft acids and bases (Pearson, 1966). It is interesting however that here

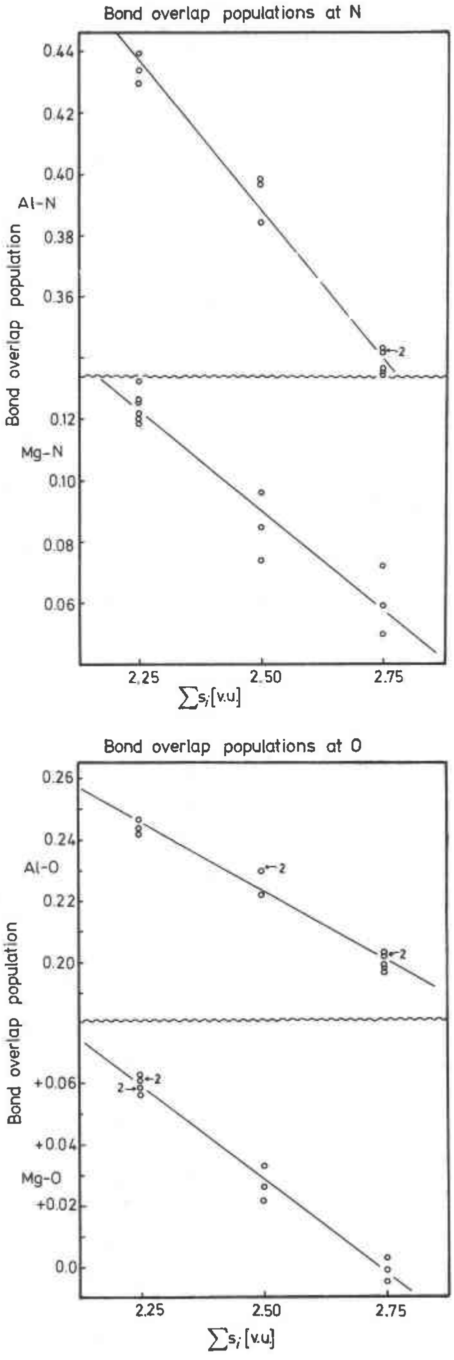

Fig. 3. The metal–anion bond overlap populations for all inequivalent bonds in the eight possible structures for MgAlON listed in Table 2, plotted against the bond strength sum at the anion. In all cases a negative correlation is predicted, in accordance with the extended valence sum rule.

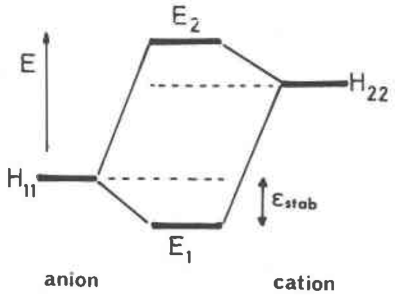

Fig. 4. Schematic orbital interaction picture showing the stabilization of the bonding orbital (largely anion centered) and destabilization of the antibonding orbital (largely cation centered).

the major driving force for (hard–soft) + (soft–hard) → (hard–hard) + (soft–soft) is the strong covalent stabilization of the soft–soft pair rather than any type of ionic interaction.

It is of interest at this stage to compare this result with the ones of Ramberg (1952) concerning the position of chemical equilibrium in metamorphic systems. From electrostatic considerations Ramberg suggested that the most stable pair of compounds for a system containing two anions and two cations of equal charge is the one where the smallest anion and cation are paired and the largest anion and cation are paired. As an example, for an ensemble composed of Be, Sr, O and S ions, the prediction (and indeed the observation) is for the stability of BeO + SrS to exceed that of BeS + SrO. This of course is the opposite result to our conclusion above *if* it were extended to this problem. However our result must be put in perspective. It is a way, borrowed from molecular chemistry of examining site preferences, and not a route for the generation of heats of formation of individual molecules or crystalline compounds. (We note, too, that Ramberg's qualification of his rule to include covalent interactions, is in the direction treated by our approach above.)

Appendix 2 develops the perturbation theoretic analysis further and demonstrates the following results:

(1) The preference for the ordering given by Pauling's rule in MgAlON does not depend on the constancy of $H_{ij}^2 S_{ij}^2$. Thus, in general in a compound containing two anion species the more electronegative anion should prefer the site of smaller Σs_i, i.e., it should prefer to have a smaller coordination number or to be coordinated by more electropositive metals.

(2) In the transformation from structures with $p_O = 2.75$, $p_N = 2.25$ to structures with $p_O = 2.25$, $p_N = 2.75$ electrons migrate away from both Mg and N toward both Al and O.

(3) In any metal–anion bond, increasing p_{anion} decreases the bond overlap population and therefore increases bond length.

(4) Anions of the same species prefer to occupy sites of equal bond strength sum, though the energetic effects driving this preference are of smaller order than those driving electronegative anions to occupy sites of lower bond strength sums than electropositive ones. That is, this effect appears only in considering second order perturbations of the anion energies, not just the first order terms discussed above.

Thus, simple perturbation arguments serve to give a complete qualitative explanation of the results derived above by more elaborate calculations with the computer. Of course, these local perturbation arguments represent simplifications of the real situation by ignoring all but nearest neighbor interactions, by passing over the effects of local geometry on these interactions, and by glossing over the fact that all four types of atoms have not one isolated valence level but an s and three p orbitals at different energies. These all introduce additional numerical complexity into the bonding picture but do not affect the validity of the perturbation arguments in broad outline. Hence the four rules stated above can be expected to be valid generally in "ionic" insulators, i.e., in solids in which atoms can be divided into "cations" and "anions" differing significantly in electronegativity and in which all close bonding interactions are between a "cation" and an anion".

Although the results of this orbital-based analysis closely parallel those of Pauling's rule and an electrostatic model, they are not identical. Because formal charge does not directly appear in our molecular orbital language we cannot comment explicitly on the numerical relation $\zeta = \Sigma s_i$. Nevertheless our rules, that anions of increasing electronegativity occupy sites of decreasing Σs_i and that identical anions occupy sites of similar Σs_i, coupled with the topological constraint that when averaged over the contents of a unit cell $\langle\zeta\rangle = \langle\Sigma s_i\rangle$, go a long way toward securing approximate numerical satisfaction of this rule. Further, as pointed out frequently (Baur, 1981a) differences of up to 40% between ζ and Σs_i are not uncommon even in stable compounds; so that an ability to predict numerical equality is not necessarily a desirable feature in the theory.

An advantage of the orbital approach over a purely ionic model is that it allows an extremely simple explanation for Baur's extended electrostatic valence rule. At the simplest level, this rule amounts to the remark that increasing the coordination number of an anion or the electronegativity of its metal neighbors ties up more and more of its electron density in these bonds and leaves less density available for bonding with another fixed neighboring atom. The perturbation argument in Appendix 2 phrases this explanation more precisely, and the detailed calculations shown in Figure 3 confirm it further. By contrast, in a simple ionic model with point charges and a spherically symmetric repulsion, the force between a pair of atoms is unaffected by neighboring atoms. Thus, a fairly complex argument involving second nearest neighbors or polarization would have to be used to explain ionically the extended valence sum rule, making it seem rather a surprise that it has the predictive power it does. The rule's extraordinary predictive power would thus seem extremely puzzling from the standpoint of the ionic model.

The most significant departure of our analysis from conventional ideas, however, lies in the replacement of formal charge with electronegativity. In most cases, increasing the formal charge of an anion decreases its electronegativity. Our rule that more electropositive anions occupy the sites of larger Σs_i then results in the same ordering as that predicted by Pauling. Where this is not the case, the two theories would make opposite predictions. Thus importantly, since nitrogen is more electronegative than sulfur despite its higher formal charge, we predict that LiSiSN and MgAlSN should not be isostructural with the analogous oxynitrides but should have structures in which $p_S > p_N$ in violation of Pauling's second rule. Synthesis of these or other compounds involving two anions in which the more electronegative has the higher charge would thus be extremely interesting.

In order to make our prediction of orderings violating the electrostatic valence rule more plausible, and at the same time to show the importance of relating mineralogy and molecular chemistry, we mention another site preference problem previously treated by us (Burdett, 1982). The As_4S_4 molecular unit found in realgar is shown in Figure 5. This is not an ionic structure since it possesses As–As bonds and 5–rings, and so the electrostatic valence rule does not help us decide which atom should occupy the two-coordinate sites and which atom the three-coordinate sites. A calculation on this molecule giving all atoms the same atomic parameters results, however, in placing more charge on the two-coordinate sites, so that these positions are predicted to be occupied by the more electronegative S atoms. This is in keeping with the general rule (which can be justified by a perturbation argument like that above) that the more electronegative atoms in a molecule occupy the site of lower coordination number.

Of course, were realgar the only such structure known, one might be tempted to argue instead, that S occupies the site of lower coordination number because of its smaller "valence". This argument would be similar to one using the valence sum rule, since in ionic compounds valence = formal charge. That this explanation is not generally valid and that the one using electronegativity is of better predictive value is seen by considering the structure of S_4N_4, also shown in Figure 5. Here nitrogen, despite its larger valence, does not occupy the As sites in realgar but the S sites, while sulfur, now the less electronegative atom, is found in the sites of higher coordination number. Electronegativity thus seems more important than valence in determining site preferences in molecules, and we predict the same should be true in more "ionic" crystals as well, as suggested by our numerical calculations.

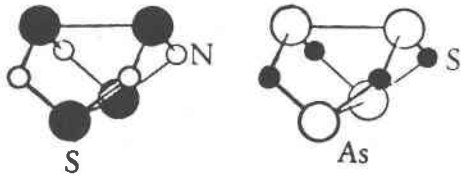

Fig. 5. The S_4N_4 and As_4S_4 (realgar) structures showing the exchange of the sulfur atom locations.

Rules 3 and 4: shared geometric elements

"The presence of shared edges, and particularly of shared faces, in a coordinated structure decreases its stability; this effect is large for cations with large valence and small coordination number, and is especially large in case the radius ratio approaches the lower limit of stability of the polyhedron." "In a crystal containing different cations, those with large valence and small coordination number tend not to share polyhedron elements with each other." (Pauling, 1929). With these two rules, the second of which is an obvious corollary of the first, Pauling moves from considering the geometry within an atom's coordination sphere to discussing systems of linked polyhedra. With these rules, too, Pauling's ionic interpretation appears most conspicuously: the absence of shared geometrical elements is attributed to the destabilizing effects of cation–cation Coulombic repulsions in structures where they occur. Numerous structures violating these rules, especially the third rule, are now known. Conspicuous examples include β-BeO (Smith et al., 1965) and the isotypic compounds $BeCl_2$, SiS_2 and SiO_2-W, all of which contain edge-sharing tetrahedra. Another striking example is the lovely dumortierite type (Moore and Araki, 1978) which has in one crystal edge-sharing octahedral chains, face-sharing octahedral chains, and octahedral chains combining edge- and face-sharing. Nevertheless, these rules are satisfied frequently enough to merit further investigation using molecular orbital methods. A preliminary account of our studies on BeO has been published (Burdett and McLarnan, 1982).

In order both to test Pauling's argument for rules 3 and 4 and to seek a covalent understanding of these rules, we have compared the observed wurtzite type structure of α-BeO with alternative structures having an h.c.p. oxygen framework but including varying amounts of edge-sharing among BeO_4 tetrahedra. Such structures can be produced from the wurtzite type by occupying some upward-pointing and some downward-pointing tetrahedra in the h.c.p. framework, instead of filling only the upward-pointing sites as in wurtzite. We have considered only those structures in which occupied tetrahedra share edges but not faces. These structures are called dipolar tetrahedral structures by McLarnan and Baur (1982) who show

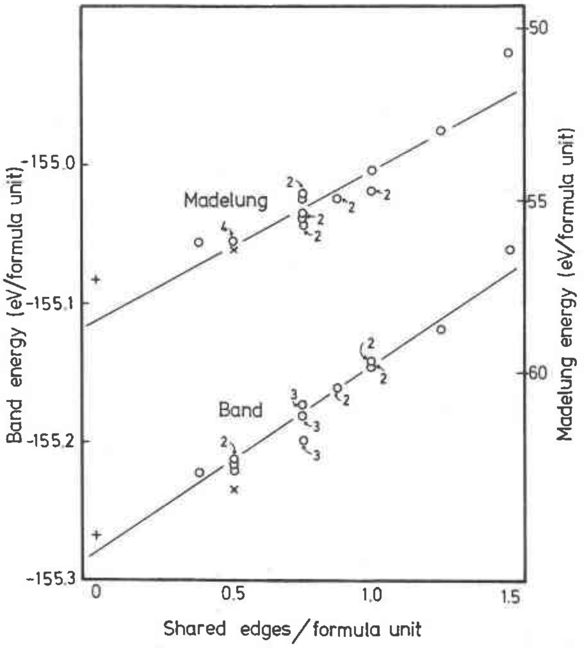

Fig. 6. The relation between number of shared edges between cation tetrahedra and both the electrostatic Madelung energy and the one-electron covalent band structure energy for 2 real observed and 21 hypothetical polymorphs of BeO. The structure types plotted are the wurtzite (α-BeO) type (cross), the β-BeO type (x) and the 21 hypothetical dipolar tetrahedral structures with (1,1) or (2,1) unit cells. The small numbers by some of the points tell how many points are represented by the single symbol.

that there are five such structures possible with a (1,1) orthohexagonal cell, and seventeen such structures with a (2,1) cell. For the composition BeO they all satisfy the electrostatic valence rule exactly, so that from the standpoint of Pauling's rules applied to idealized structures with all tetrahedra regular, they should differ in energy only because they differ in amount of edge-sharing.

Figure 6 shows the energies of these twenty-two structures plotted as a function of the number of shared edges. In this plot we have evaluated the energy both using our covalent band structure calculations and using a pure point charge Madelung sum (i.e., $E = 1/2\ \Sigma(q_i q_j / r_{ij})$, where q_i and q_j are the charges on atoms i and j separated by a distance r_{ij}), the most extreme and simple ionic model. As can be seen, in both cases the energy can be described accurately as a linear function of the number of shared edges, in keeping with Pauling's third and fourth rules. Thus, either a purely electrostatic or an essentially purely orbital model predicts that counting shared edges is nearly equivalent to working out total energy. Of course, the two methods have different standard states, and both produce meaningful relative energies but not meaningful absolute energies; so one would not expect either the intercepts or the slopes of the two lines to be equal.

Electrostatic interactions fall off very slowly with distance (they diminish as 1/r), so one might well imagine that the Madelung energy of a crystal should be poorly predicted from a knowledge of purely local geometry. The high degree of linearity in the plot of Madelung energy vs. shared edges ($r^2 = 0.869$) is thus actually a surprise. Overlap interactions fall off much more rapidly than electrostatic (at least as $1/r^3$), but this fact alone obviously does not explain the observed linear relation ($r^2 = 0.959$) between number of shared edges and band structure energy.

To understand the variation in covalent energy, it is natural to consider first the atoms on which the majority of the electron density resides, that is, the anions. In these twenty-two crystal structures there are four possible anion coordination geometries, which are shown in Figure 7a. These geometries are numbered 0, 1, 2 and 3, the numbers indicating the number of shared edges in which an anion in that configuration participates. The energetic effects of these different geometries can be assessed by computing the energies of eight-electron OBe_4^{+6} "molecules" via Extended Hückel calculations of the molecular type. For conceptual simplicity and in order to model better the crystal calculations which place very little electron density on the metal atoms, we employ pseudoberyllium atoms having only *s* orbitals in these calculations. The parameters are listed in Appendix 1, and the energies are given in Table 4.

Given these values, approximate energies for the twenty-two crystal structures can be computed by simply

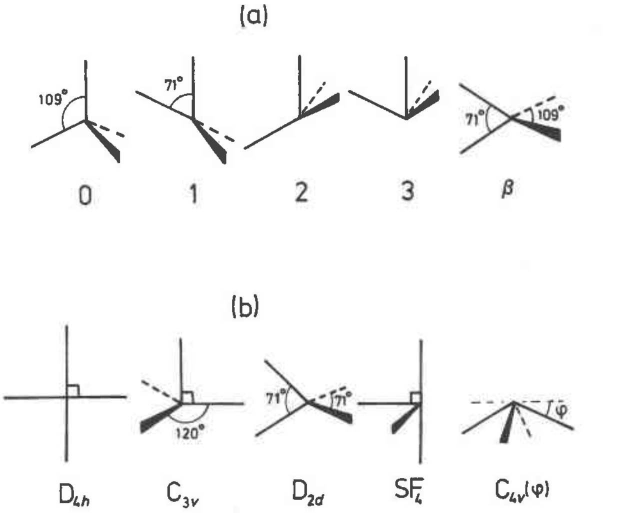

Fig. 7. (a) The five different oxygen coordination environments found in the 23 structure types in Fig. 6. Conformation 0 is a regular tetrahedron. Conformations 1, 2 and 3 are derived from a tetrahedron by replacing tetrahedral angles $\theta = 109.47°$ with angles of $180°-\theta$ between 1, 2 and 3 pairs of bonds, respectively. Arrangement β, found only in β-BeO, has local symmetry *mm*2, as shown. (b) Five other possible molecular geometries for OBe_4.

Table 4. Energies and overlap populations in OBe_4 Molecular Units[a]

"Molecule"	E(eV)	E'(eV)	Bond Overlap Populations <Be-O>	<Be-Be>
0	0	0	0.0935	-0.0049
1	0.0255	0.0162	0.0905	-0.0039
2	0.0654	0.0469	0.0863	-0.0032
3	0.1221	0.0930	0.0803	-0.0028
β	0.0201	0.0117	0.0911	-0.0040

[a] The relative energies E of the 5 different OBe_4 "molecules" in Figure 7. The energies E' for the same molecules are computed after dropping all direct ligand-ligand interactions. The average Be-O and Be-Be bond overlap populations refer to the calculation including these interactions.

taking $\Sigma n_i E_i$ where n_i is the number of anions per unit cell having coordination geometry i, and E_i is the energy of this geometry from Table 4. As can be seen in Figure 8, this calculated energy obtained from "molecular" fragments and the crystal energy from the full band structure computation agree extraordinarily well ($r^2 = 0.994$). The slope of Figure 8 is not exactly unity, since the local geometries have been energetically modelled by taking s orbitals alone on the ligands. (Use of the valence *s* and *p* orbitals on the Be atoms does not improve the situation. An accurate numerical representation could be obtained by ensuring a realistic ligand environment, which can only be achieved in the crystal itself). Crystal energies are then, to a first approximation, the sums of energies associated with the anion coordination environments. However we cannot completely exclude an extra orbital effect, increasing with the number of shared edges, and transmitted through the bridging oxygen atoms, since we have no means of knowing whether the variations in the local geometry sum numerically accounts for all of the calculated variation in the band structure energy. With this qualification we develop the idea that increasing the number of shared edges, increases the number of less stable anion coordination environments.

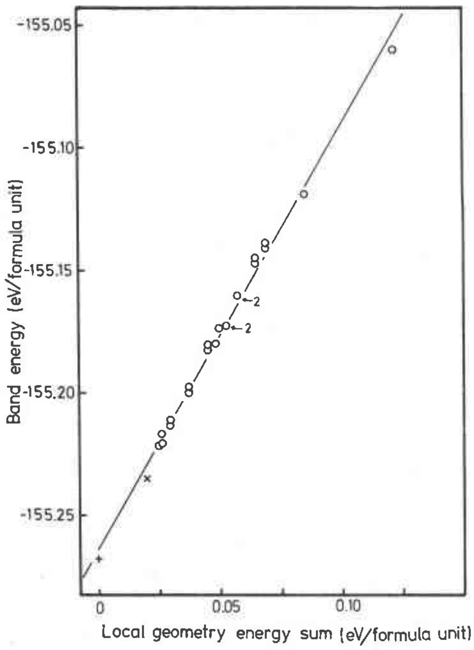

Fig. 8. The correlation between the one electron band structure energy of BeO polymorphs and an energy computed by adding local contributions from each anion coordination polyhedron. Energies of the 5 possible local environments (Fig. 7) are found from calculations on OBe_4^{+6} "molecules." The structures plotted and meaning of symbols are as in Fig. 6. The small numbers by some of the points tell how many points are represented by the single symbol.

As a further test of the importance of anion coordination, we consider the structure of β-BeO (Smith et al., 1965) shown in Figure 9. This material is a three-dimensional framework composed of edge-sharing Be_2O_6 dimers which then link by vertex-sharing. The oxygen atoms are not closest-packed but form the less dense rutile packing of Baur (1981b). If the BeO_4 tetrahedra in this arrangement are taken to be regular, as in the twenty-two dipolar tetrahedral structures above, then the coordination about the anions is that shown in Figure 7. An OBe_4 molecule with this geometry lies below any of the conformations 1, 2 and 3 in energy (Table 4), and as shown in Figure 6, the three-dimensional β-BeO crystal structure lies lower both in one electron orbital energy and in Madelung energy than any of the twenty-two types above except that of wurtzite (α-BeO). This occurs despite the fact that four of the twenty-one higher energy types have the same number of shared edges as β-BeO, and one has fewer. As shown in Figure 8, the energy of β-BeO relative to α-BeO is well approximated by the same linear expression based on the relative energies of the constituent OBe_4^{+6} molecules which applied to the dipolar tetrahedral structures. Thus, anion coordination geome-

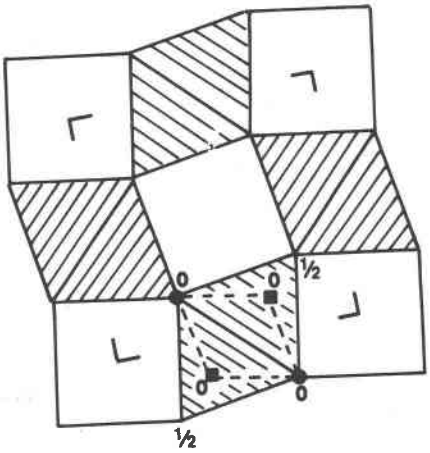

Fig. 9. Idealized crystal structure of β-BeO. Shaded rhombuses are pairs of edge-sharing BeO_4 tetrahedra seen down z. The dashed lines show one of the planar four-membered rings composed of 2 Be atoms (squares) and 2 O atoms (circles).

try alone can enable one to rank energetically even sufficiently similar structure types with different anion packings. It can further help to rationalize the occurrence of structures like β-BeO with more shared edges (but also more stable anion environments) than some unobserved alternatives. We shall return to the β-BeO structure in discussing shared edge shortening and nonbonded repulsions.

Although our analysis thus arrives at the same conclusion concerning the lowest energy structure as does an ionic interpretation, it is important to stress that it does so for very different reasons. In particular, the different anion coordination geometries do not differ in energy because of increased cation–cation repulsions at the tighter Be–O–Be angles. Instead the energy differences are due almost entirely to the ability of the central oxygen atom to form stronger bonds when its coordinated Be atoms are arranged tetrahedrally. This can be seen from several arguments.

First, one can consider the various bond overlap populations in molecules 0–3. As can be seen from Table 4, the average Be–O bond overlap population increases for the more stable molecules, and the correlation of energy with Be–O bond overlap population for these molecules is nearly exact ($r^2 = 0.9997$). The Be–Be bond overlap population not only has a poorer correlation with the total energy ($r^2 = 0.8765$), but correlates the wrong way: the higher energy molecules have less total Be–Be repulsion as measured by average bond overlap populations. Thus, while Be–Be interactions contribute a net destabilization to all of these molecules, that destabilization is reduced by bringing the Be atoms closer together. This is not surprising when one considers that the Be atoms are extremely electron poor, so that bringing them together enhances small bonding interactions between them. So, decreasing molecular stability in the sequence 0, 1, 2, 3 is dominated by poorer Be–O bonding (measured by smaller O–Be bond overlap populations), with a slight counterbalancing effect due to Be–Be attractions (measured by less negative Be–Be bond overlap populations).

Perhaps an even stronger argument for this point of view in the molecular case is provided by the data in the third column of Table 4. This shows the relative energies of the four molecules determined by a calculation in which all overlap integrals and Hamiltonian elements between different Be atoms were set equal to zero. In this calculation the ligands can feel only the central atom, not one another. Despite this, the energy differences in this calculation are proportional to and nearly as large as those in the calculation including ligand–ligand overlaps. Thus, at most a small percentage of the differences can be caused by metal–metal interactions. Whether the decrease in Be–O bonding, as the geometry distorts away from tetrahedral, is due to a change in s–p mixing (Burdett, 1979) or occurs via a change in overlap between predominantly oxygen $2p$ orbitals and the ligands (Burdett, 1976) in a question we shall not tackle here. That the total one-electron stabilization energy associated with oxygen–beryllium orbital interactions decreases on distortion is, however, unequivocal.

Table 5. Energies and overlap populations in solid BeO variants[a]

Structure	Energy (eV)	Bond Overlap Population Sums Be-O	Be-Be	O-O
wurtzite	-621.047	3.2736	-0.4728	-0.0864
D-Pmnn(1,1)	-620.867	3.1728	-0.4228	-0.0816
D-Pm 11(1,1)	-620.674	3.0784	-0.4170	-0.0783
D-Pmcn(1,1)	-620.575	3.0096	-0.4032	-0.0772
D-$P\bar{3}mc$(1,1)	-620.218	2.8640	-0.3696	-0.0690

[a] The energies per 8 atom unit cell and the total first and second neighbor bond overlap populations per cell of the five dipolar tetrahedral structures with (1,1) unit cells.

Finally, it is possible to apply our reasoning about bond overlaps directly to the crystal structures themselves. Table 5 shows the energies and Be–O, Be–Be and O–O bond overlap populations of the five possible BeO structures with a (1,1) cell. These were computed using the results of band structure calculations on the infinite crystals and not from molecular calculations on finite molecules. The Be–O bond overlaps have been summed over all Be–O bonded contacts in one unit cell, the O–O populations represent similar sums over all pairs of O atoms coordinated to one another in the h.c.p. oxygen lattice, and the Be–Be populations are sums over all pairs of Be atoms bonded to a common oxygen atom. Just as in the molecular case the total energies are extremely linear in the Be–O bond overlap population ($r^2 = 0.994$), as shown in Figure 10. The Be–Be interactions again become less antibonding in the less stable structures, and vary much less than the Be–O interactions. Further, in a multiple linear regression these interactions explain only 6% of the energy variation not attributed to linear dependence on the Be–O bond population. Be–Be interactions thus play only a slight role in the total crystal energy. The same is true of the even smaller O–O interactions. Thus, the orbital model does not in this situation bear out the traditional explanation given for Pauling's third and

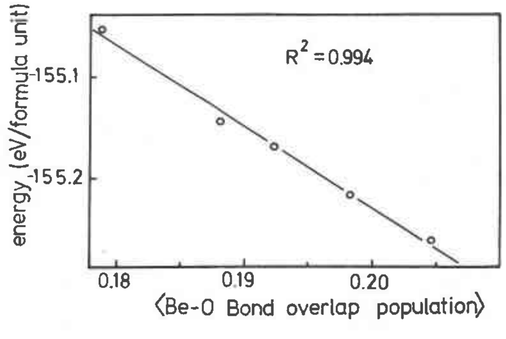

Fig. 10. The correlation between average Be–O bond overlap population and the one-electron band structure energy for the wurtzite structure and dipolar tetrahedral structures of Table 5.

fourth rules, even though it agrees with these rules' predictions.

Why then are the results of the Extended Hückel calculations so strongly correlated ($r^2 = 0.935$) with those of Madelung calculations for our twenty-two possible BeO structures? To answer this question, we must first consider why these structures have different Madelung energies. The fixed h.c.p. oxygen framework in these structures guarantees that every anion sees the same site potential due to neighboring anions in all twenty-two structures. Further, every anion in any one of these structures has the same number of cations at any given distance as any other anion, so the contribution of cation–anion interactions to the Madelung energy will also be identical throughout these types. They will differ in energy only because of cation–cation repulsions. The strong correlation between Madelung energy and shared edges suggests that repulsions between neighboring cations account for most of the energy differences. Thus, an approximation to the Madelung energy could be obtained by evaluating the cation-cation repulsions in molecules 0–3. This is simply

$$\frac{1}{2}\sum_{i,j=1}^{4}\frac{4}{r_{ij}}.$$

The total one-electron energy of these molecules, however, is very surprisingly also proportional to

$$\sum\frac{1}{r_{ij}}.$$

This is shown in Figure 11, which plots energy as a function of

$$\sum\frac{1}{r_{ij}}$$

not only for molecules 0–3 but for a number of other arrangements (Fig. 7) of four Be atoms around a central oxygen. These include both fairly regular and extremely distorted geometries. In this plot we have dropped all interactions between pairs of Be atoms in order to guarantee that we are seeing a covalent effect unrelated to Be-Be repulsions, but an identical correlation results if these interactions are retained.

The origins of this remarkable proportionality (suggested to us by Dr. T. H. Upton) which plainly lies at the heart of the agreement between the covalent and ionic models in their energetic predictions on this family of structures leads to a problem in molecular stereochemistry which is at present unresolved. As already stressed, the result is not a reflection of Be–Be repulsions. Rather the molecules behave as if there were localized hybrid orbitals pointing to each of the ligands, and as if these bonding hybrids interacted purely by electrostatic repulsion.

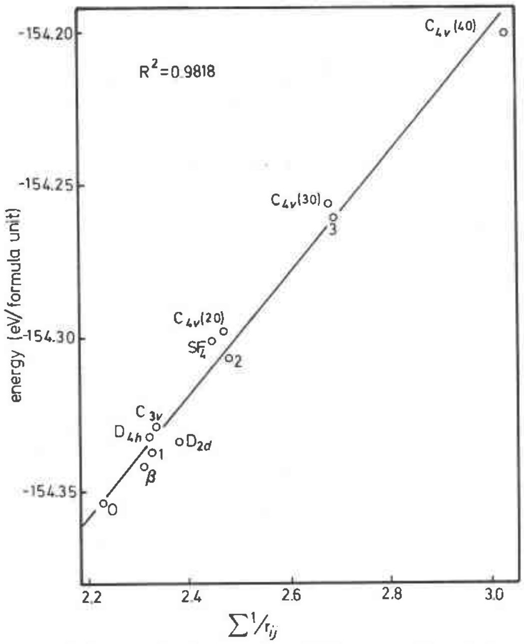

Fig. 11. The covalent energies of 11 different conformations for a molecule OBe_4^{+6} as a function of the sum of the Be–Be distances. The 11 geometries are shown in Fig. 7.

The geometrical implications of this result are thus identical to the predictions of the familiar valence shell electron pair repulsion (VSEPR) model (Burdett, 1980; Gillespie, 1972) which attempts to explain molecular geometries as resulting from so-called "Pauli repulsions" between localized pairs of electrons about a central atom. If these pairs repelled one another entirely by Coulombic forces, the energy predicted by VSEPR would be proportional to

$$\sum\frac{1}{r_{ij}}$$

and hence parallel to the variations in the one-electron molecular orbital energy. The VSEPR approach can be codified and applied to dynamic problems in the so-called points-on-a-sphere (POS) model (Bartell and Plato, 1973; Bartell, 1984). Here ligand atoms are treated as points at a constant distance from a central atom which interact via repulsive forces to give an energy of $\Sigma\ 1/r_{ij}^n$ for some n. Physically, these interactions are presumed to include hybridization effects, ligand–ligand steric repulsion, electrostatic forces and "Pauli forces" between bond pairs. Using these assumptions the observed vibrational force constants may be used to fix the value of n. For molecular PF_5 it appears that the repulsions may be much harder than those seen in the "ionic" case here ($n \simeq 7$). This may be caused by the large nonbonded repulsions between the electron-rich, closed shell, fluorine atoms compared with weak attractive interactions between the electron-poor Be atoms in OBe_4^{+6}. If n were not close to 1 in OBe_4, Madelung calculations alone would not provide a means of computing relative energies of our BeO polymorphs, though a more complex ionic model incorporating a $1/r^n$ repulsive force might apply. Also it has not escaped our attention that PF_5 is a much more "covalent" system than OBe_4^{+6}. Molecular orbital calculations for hypothetical octet AX_4 systems show that the law of force between the ligands, or bond pairs hardens quite dramatically as the electronegativity difference between A and X decreases. This may well be the reason for the failure of Madelung type ideas in general to predict the most stable structure in more "covalent" materials.

Finally, we comment on the relation between our ideas and Pauling's (1960) own valence bond interpretation of molecular structures. We predict that shared edges are destabilizing because they result in distorted anion coordinations and hence weaker metal–oxygen bonding. This argument is quite similar to that used by Pauling to explain the tetrahedral structure of methane. This structure is found not because of H–H repulsion but because the tetrahedral arrangement enables strong sp^3 bonding hybrids to form. Indeed both Pauling-type generalized valence bond (GVB) calculations (performed by Dr. T. H. Upton) and Extended Hückel calculations predict methane to be tetrahedral, and the two methods agree numerically to within 7% in their predictions of the energy differences among molecules CH_4 in configurations 0, 1, 2, and 3 (Table 6). Unfortunately, GVB calculations can be applied neither to highly ionic molecules like OBe_4^{+6} nor yet to solids, but the qualitative argument that four-coordinate eight electron anions should seek to form sp^3 hybrids and hence should prefer a regular tetrahedral geometry remains. Interestingly, in his original paper on rules for ionic solids, Pauling (1929) implicitly uses this argument by rationalizing the six-membered rings in beryl as making the Si–O–Si angle close to the tetrahedral angle of 109°. In a purely ionic compound this angle should prefer to open to 180°. By and large, of course, Pauling employed ionic ideas in dealing with solids, but it is startling to see how applying modern ideas of electronic structure to "ionic" crystals results in an interpretation of their geometry which is largely convergent with that pioneered by Pauling in the molecular realm.

The important role we have assigned here to anion coordination geometry and our almost total neglect of cation coordination is not by any means new to us. Wells (1975), O'Keeffe and Hyde (1982), Caro (1968, 1972), and Franzen (1966)) among others have all pointed out the importance of anion coordination in explaining a number of otherwise complex structure types. The concentration of O'Keeffe and Hyde (1978, 1981, 1982) on anion coordination and cation–cation distances is particularly close to our view of the importance of bond angles at the anions. Nevertheless, the tradition of reporting and considering only cation coordinations, though condemned already by Bragg (1930), is still alive. Crystallographers should therefore again be reminded that not every structure type is best described or explained by ignoring the environment of half the atoms and most of the valence electrons.

Table 6. Relative energies (eV) of CH_4 molecules in the geometries O-3.

	Extended Hückel	Generalized valence bond [a]
0	0	0
1	1.349	1.390
2	2.657	2.630
3	3.894	3.642

[a] Calculations performed by Dr. T.H. Upton

Rule 5: parsimony

"The number of essentially different kinds of constituents in a crystal tends to be small." (Pauling, 1929.)

It is not obvious that this rule bears a particularly close connection to any particular energetic model, and it has not been frequently addressed in the literature after 1929. Bragg (1930) regarded it as a corollary of rule 1 (which limits variation in cation coordination number) and rule 2 (which combined with rule 1 limits the number and type of cations about each anion). While this rule is not intended to imply that essentially equivalent constituents must be crystallographically equivalent, it is certainly related to the more fundamental observation that most common materials are crystalline rather than amorphous. This at least guarantees that the number of essentially different kinds of constituents of a material will be finite rather than infinite.

We have little insight as to why either of these rules should be the case beyond the fact that they are consequences of the short-range nature of interatomic potentials. (Consider, for example, an assemblage of balls connected by springs which would at equilibrium possess a periodic arrangement). Covalent forces in the Extended Hückel approximation fall off much more rapidly than electrostatic forces (energies decrease at least as r^{-3} rather than r^{-1}). Further, the perturbation arguments carried out in Appendix 1 and alluded to above have shown that orbital interactions operating solely between nearest neighboring atoms act to favor identically coordinated anions. To what degree observation demands these extremely short range forces rather than much longer range ionic interactions is by no means obvious, however. Indeed one of the more difficult problems for either the covalent or ionic model to resolve is how ordered structures with extremely large unit cells (e.g., 1500Å dimension *c* in some polytypes of SiC (Shaffer, 1969) can be produced even by electrostatic forces.

Finally, it is interesting that Baur et al. (1983) have developed a numerical index for the degree of parsimony in a crystal structure, and have shown that using this measure many crystal structures are not parsimonious but lavish in their use of different local environments.

Shared edge shortening and nonbonded repulsions

Pauling's five rules deal entirely with structures possessing idealized regular cation coordination polyhedra. In the remaining portion of his paper (Pauling, 1929), however, he states an extremely useful consequence of the electrostatic model of crystal energies, namely that shared edges between cation coordination polyhedra should be shortened because of metal–metal Coulomb repulsions. More recently O'Keeffe and Hyde (1978, 1981, 1982) have argued that many features of crystal structures can be explained by very hard metal–metal repulsive potentials resulting in cations behaving essentially as hard spheres with large and constant nonbonded radii.

Shared edge shortening has been investigated extensively using molecular orbital methods of widely varying degrees of sophistication (see references in Gibbs et al., 1981). These studies have invariably employed molecules or "molecular" fragments torn from crystal structures, but have almost always produced results in close agreement with observation (one exception being a CNDO/2 study of Mg_2SiS_4, the sulfide analogue of forsterite (McLarnan et al., 1979).

To see qualitatively how nearest neighbor covalent forces might produce shared edge shortening even in the absence of direct metal–metal interactions, consider the coordination polyhedra about the anions in a dipolar tetrahedral structure with only one shared edge in each MO_4 tetrahedron. This local geometry is shown in Figure 12. It is obvious that shortening the O–O distance in the shared edge while maintaining a constant M–O distance results in more regular OM_4 tetrahedra. Such a distortion should therefore be favored by the anion hybridization effects which were used above to explain the energetic differences among dipolar tetrahedral structures with regular cation coordination tetrahedra. Indeed, one might expect that in the total absence of nonbonded interactions, the requirements of anion hybridization would lead to a configuration in which the OM_4 tetrahedra were exactly regular and the MO_4 tetrahedra suffered extreme distortions (in particular, they would have one O–M–O angle of 70.53°). Thus, shared edge shortening certainly does not imply direct metal–metal repulsions.

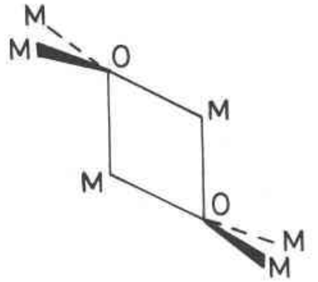

Fig. 12. The local coordination geometries about the two oxygen atoms composing a shared edge in a dipolar tetrahedral structure.

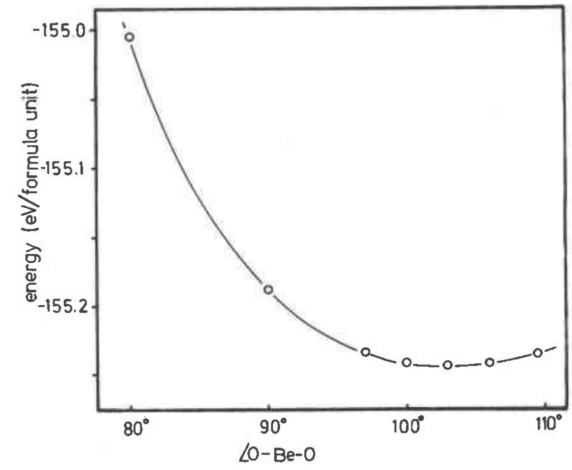

Fig. 13. The calculated energy of β-BeO as a function of the O–Be–O angle at the shared edges.

To render this argument more quantitative, to study the roles of M–M and O–O interactions in shared edge shortening, and to understand why observed structures do not show the extreme distortions of cation coordination polyhedra predicted from hybridization effects above it is necessary to carry out some calculations. The obvious choice of structure on which to perform these is β-BeO (Fig. 9), both because it is observed and because it can be distorted to give the O–Be–O angle at the shared edge any desired value without changing any of the Be–O distances. Details of the distortion pathway are described in Appendix 1. An additional advantage of β-BeO is that if the O–Be–O angle in the 4-rings (and consequently the Be–O–Be angle as well) is set equal to 90°, a structure results which is its own antistructure. That is, interchanging the Be and O atoms produces a geometrically identical crystal. This self-complementary arrangement is that predicted by a pure Madelung calculation. Thus, distortions from O–Be–O = 90° can be used to measure the relative importance of Be–Be repulsions (which would tighten this angle) and O–O repulsions (which would open it). Of course, hybridization effects around the anions will also prove important here.

The one-electron energy of β-BeO as a function of the O–Be–O angle at the shared edge is shown in Figure 13. As can be seen, a shortening of the shared edge is predicted, and the calculated O–Be–O angle of 103.3° is in acceptable agreement with the observed value of 98.4° obtained from powder data (Smith et al., 1965).

The explanation for this calculated bond angle can be seen in Figure 14, which shows the variation with O–Be–O angle of (1) the Be–Be and O–O bond overlap populations across the ring, and (2) the average of the O–Be bond overlap populations at each oxygen. This shows that there are two effects acting to open the O–Be–O angle. First, there are cross-ring O–O repulsions between the nearly filled shell oxygen atoms, and second there are

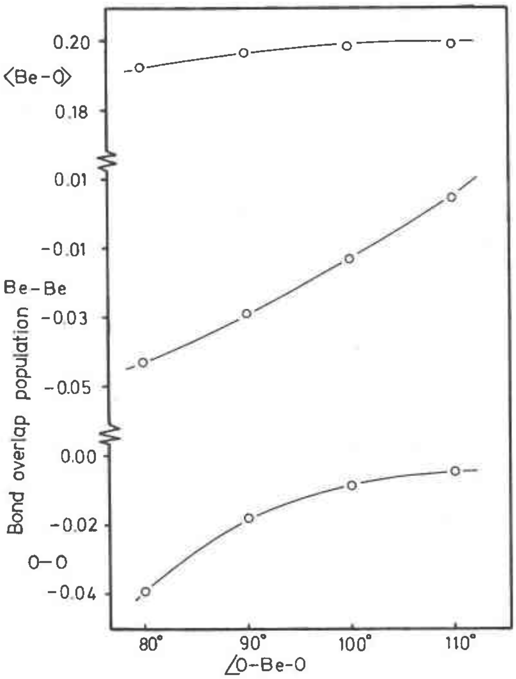

Fig. 14. Calculated average bond overlap populations between bonded atoms and between the nonbonded metal and oxygen atoms at the shared edge in β-BeO.

cross-ring Be–Be *attractions* between the extremely electron deficient beryllium atoms. This attractive interaction between the metal atoms means that the observed angle cannot be viewed as a balance between O–O and Be–Be interactions, since these both act to enlarge the angle O–Be–O. The balancing energetic contribution acting to decrease this angle is the preference of the oxygen atoms for tetrahedral OBe_4 coordination. This effect is not clearly shown by the trend of the O–Be bond overlap population, but its importance in the total energy of both crystal and molecular tetrahedral structures has been amply demonstrated above by examining rather simpler structure types than β–BeO.

In order to confirm the importance of O–O repulsions and Be–Be attractions and to attempt to weigh their relative magnitudes, we repeated these calculations "turning down" first the O–O interaction and then the Be–Be interaction by artificially halving all O–O (or Be–Be) overlap integrals. In both cases the O–Be–O angle shrank, as expected if O–O interactions were repulsive and Be–Be ones attractive. The change in equilibrium angle was, however, small (1.8° when O–O interactions were reduced and 1.5° when Be–Be were reduced). This suggests that either the Be–Be attractive potential or the O–O repulsive potential must be quite hard (presumably the latter). Further, it hints that while both Be–Be attractions and O–O repulsions affect the equilibrium geometry, the O–O interactions may be somewhat more important. This is borne out by the bond overlap populations plotted in Figure 14. The greater electronegativity of oxygen means that changes in O–O bond populations have a larger energetic effect than comparable changes in those for Be–Be. All these conclusions might be strengthened by reducing nonbonded interactions further still; but unfortunately, attempting this results in an ill-conditioned Hamiltonian matrix.

The interpretation that shared edge length represents a compromise between short anion-anion edges favored by anion hybridization effects and long edges favored by anion-anion repulsion and cation-cation attraction is obviously at odds with the conventional electrostatic model. It is also at odds with O'Keeffe and Hyde's (1978, 1981, 1982) view that crystal geometries are largely determined by a very hard repulsive cation–cation potential, of which we see no trace. Both these other interpretations, result in incorrect geometric predictions for β-BeO. A pure point charge model leads to an O–Be–O angle of 90°. A model in which metal–metal repulsions dominate O–O repulsions should result in d(Be–Be) > d(O–O) in the 4 rings, so that O–Be–O < 90°. Some indication of the failure of this second approach is shown in Table 7, which compares metal–metal and O–O distances in β–BeO and two of its derivatives with the sums of the "one angle" nonbonded radii from O'Keeffe and Hyde (1981). Let us state first of all that our use of these "one angle" nonbonded radii is technically incorrect since they are not designed for such square environments but much more open ones. However, we have used these values for lack of anything better to represent that ill-defined quantity "nonbonded radius." As can be seen, the oxygen atoms are well over two radii apart, but the metal–metal separation averages 0.42Å less than the sum of the nonbonded radii.

Thus, our energetic interpretation is novel, and the covalent approach, unlike models based on point charges or fixed nonbonded metal–metal distances, produces

Table 7. Geometric data in β-BeO and derivatives[a]

Compound	Distance	Radius sum	Observed
β-BeO [a]	Be-Be	2.70	2.20
β-BeO	O-O	2.24	2.55
γ-$LiAlO_2$ [b]	Li-Al	3.12	2.66
γ-$LiAlO_2$	O-O	2.24	2.74
γ-Li_2BeSiO_4 [c]	Li-Be	2.85	2.50
γ-Li_2BeSiO_4	Li-Si	3.03	2.64
γ-Li_2BeSiO_4	O-O	2.24	2.60
γ-Li_2BeSiO_4	O-O	2.24	2.61

A comparison of metal-metal and O-O nonbonded distances across the 4-rings in β-BeO and two of its derivatives with the nonbonded radii of O'Keeffe and Hyde (1981),

a. (Smith, Cline and Austerman (1965))

b. (Howie and West (1974))

c. (Marezio (1965))

qualitatively correct behavior in the 4-rings (d(Be–Be) < d(O–O)), and indeed makes a quantitatively acceptable prediction of the O–Be–O angle.

Lower anion coordination numbers

In all the compounds discussed so far, the anions have coordination number four, and hence prefer a tetrahedral environment, just as they would in the electrostatic model. With lower coordination numbers, however, the predictions of the two models diverge further. A pure point charge model would predict that a molecule like NH_3 should be planar and that H_2O should be linear, since in these conformations the cation–cation distances are maximized. Molecular orbital arguments, however, lead to the correct prediction that both these molecules should be bent. To a first approximation, the hydrogen atoms should occupy 2 or 3 of the vertices of a tetrahedron, with lone pairs of electrons pointing toward the remaining vertices. This prediction is made either by simple arguments from perturbation theory or Walsh diagrams (Burdett, 1980) or using traditional electron counting methods (Gillespie, 1972).

Numerical calculations of the extended Hückel type reproduce poorly the geometries of two and three coordinate molecular hydrides but appear to be reliable for nonhydrides. There is also evidence however that, as the electronegativity of X decreases, a long way below that of A in an AX_n system with $n = 2, 3$ then the linear and trigonal planar geometries respectively are the ones expected on both orbital and electrostatic reasoning. Molecular examples however are few; linear Li_2O is one known experimentally as a gas phase molecule, but calculations have been performed on many unknown molecules of this type (Dill et al., 1977). $LiNH_2$ is one such species, predicted to be pyramidal by VSEPR but computed to be most stable at the planar structure. The electronic factors influencing the stabilities of the two geometries will be finely balanced, involving ionic and covalent contributions to the energy.

In view of this difficulty, we must be careful in using band structure calculations to study the local anion geometries in solids with two- and three-coordinate anions. It is interesting however, that an informal survey of binary halide crystal structures with two- and three-coordinate halogens shows that pyramidal or bent anion configurations occur in a substantial majority of these structures. The exceptions are nearly all very ionic fluorides. A preference for bent or pyramidal coordination does not imply massive violation of the third and fourth rules, since a tetrahedral bond angle at the anions is sufficient to preclude the sharing of, say, tetrahedral edges or octahedral faces without substantial distortion. Of course, bent configurations are known to be often found at the oxygen sites in silicates, for example. (Tossell and Gibbs, 1978; Newton, 1981; Gibbs et al., 1981).

Despite its shortcomings, the Extended Hückel method can still be employed to study energetic differences among structures having two- or three-coordinate anions as long as all the anion sites in the structures in question have substantially identical nearest neighbor environments (e.g., all planar or all pyramidal). We have done this, for example in a study of structures related to arsenic with pyramidal three-coordination (Burdett et al., 1981). We sketch here the broad results of a study of the structures of rutile and α-PbO_2. If these structure types are idealized by regarding them as based on ideal hexagonal close packing of the anions, as shown in Figure 15, then the anions in both structures have the nearly planar Y-shaped coordination environments of Figure 16. Band structure calculations using these idealized structures with Si and O atomic parameters and with d(Si–O) set equal to that in stishovite (rutile-type SiO_2) places the rutile type significantly lower in energy than α-PbO_2, as

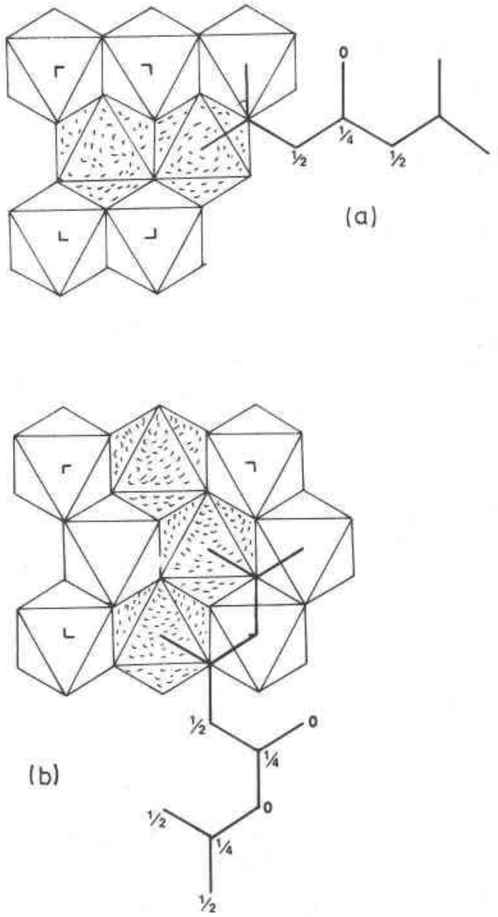

Fig. 15. Idealizations of the crystal structures of rutile (a) and α-PbO_2 (b), where both structures are regarded as having ideal h.c.p. anion-arrays. Stippled octahedra are occupied by cations at $z = 1/2$; unstippled octahedra have cations at $z = 0$. Also shown are fragments of the two different infinite M_2X (M = cation, X = anion) chains which make up these structures. In these chains, 3-coordinate atoms are anions and the other (bridging and terminal) atoms are cations.

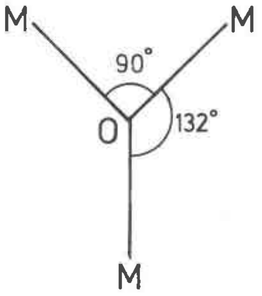

Fig. 16. The oxygen coordination environment in the idealized rutile and α-PbO_2 structures.

expected. Both rutile and α-PbO_2 can be formed by fusing together chains of composition Si_2O which are shown in Figure 15. These chains are chosen to be the simplest ones that contain all of the silicon atoms which coordinate a given chain oxygen atom. The Si_2O chains in the two structure types are inequivalent; those in α-PbO_2 represent twisted versions of those in rutile. The difference in the energy per oxygen atom in these two chains, treated as 1-dimensional crystals, is nearly exactly equal to the difference in energy per O atom we computed in the 3-dimensional crystal structures themselves. Thus, to compare the energies of these two structures, it is sufficient to compare the energies of the constituent chains. It is possible to understand the energetics of these two chains by looking at individual orbitals at various points in *k*-space, but the analysis is complex and will not be presented here. Notice however that the chains we consider are not the octahedral edge-sharing (SiO_4) chains which would first occur to a crystallographer looking at the cation coordination in these structures, but are based instead on the anion coordination environments. As should be expected, the energies of the octahedral (SiO_4) chains, in which the electron-rich O atoms have their coordination environments disrupted, do not match the energies of the two 3-D structures. This illustrates again the extreme importance of anion coordination in determining "ionic" crystal structures. It is interesting that we have not been able to understand the energy differences between rutile and α-PbO_2 by using small "molecular" fragments like the OBe_4 units used above, but this time have been compelled to consider infinite chains as our building blocks. We suggest that an orbital interpretation of solids with 2- and 3-coordinate anions in general should be accessible using similar ideas.

Conclusions

We summarize our major conclusions.

1. Pauling's first rule predicts coordination numbers badly, even for the alkali halides. Far superior sorting of structures can be obtained using pseudopotential radii, which are correlated with both atomic size and electronegativity. (This comes from earlier work; see Burdett and Price, 1981).

2. The valence sum rule has a large topological component. Much of the nontopological content of this rule can be understood to follow from the conclusions of perturbation theory. Electronegative anions tend to be coordinated by electropositive cations and vice-versa, and identical anions prefer similar environments. In hypothetical compounds such as LiSiSN in which the more electropositive anion has a lower formal charge, perturbation theory and the valence sum rule make opposite site preference predictions. The orbital interpretation, unlike the ionic model, yields a simple explanation for the extended valence sum rule.

3. Cation coordination polyhedra in tetrahedral compounds tend not to share geometric elements because structures with edge or face sharing have distorted anion coordination environments which result in poor anion hybridization and weaker metal–anion bonds. The energy of a distorted tetrahedral OM_4 "molecule" is proportional to $\Sigma 1/r_{ij}$, where r_{ij} runs over all metal–metal distances in the molecule. This proportionality helps to explain the success of the electrostatic model and Madelung calculations in general.

4. Shortened shared edges between cation coordination polyhedra arise from a balance between anion hybridization effects (favoring short edges) and both anion–anion repulsion and, to a lesser degree, cation–cation attraction (favoring long edges). Nonbonded metal–metal repulsion does not play a significant role.

Thus, molecular orbital ideas allow one to reinterpret Pauling's classic rules in terms more compatible with modern ideas of bonding than the original electrostatic model. The reinterpretation bears out many of Pauling's predictions and allows some others to be modified to fit better the results of the past fifty years of structural research. Like any simple model, qualitative or approximate, our molecular orbital methods represent an approximation to the precise quantum mechanical truth. Nevertheless, this approximation has proven tremendously productive in understanding molecular structures. It is thus pleasing indeed to one believing in the unity of nature that such methods have something to say about crystals as well.

Finally, there is a nice symmetry in an understanding of Pauling's rules based on the very ideas of orbital hybridization and covalent interactions which Pauling himself pioneered in the study of molecules.

Acknowledgments

We would like to thank Dr. T. H. Upton (Exxon Research Laboratories) for performing the GVB calculations on CH_4 and making some very pertinent suggestions as to the origin of the results of Figure 6. We also thank Professor W. H. Baur, Professor J. D. Corbett and Professor M. O'Keeffe for their input concerning the crystal chemical principles involved. Acknowledgement is made to the donors of the Petroleum Research Fund administered by the American Chemical Society for their partial support of this research. This research was also supported by the National Science Foundation by NSF DMR8019741.

References

Baldereschi, A. (1973) Mean-value point in the Brillouin zone. Physical Review, B7, 5212–5215.

Bartell, L. S. and Plato, V. (1973) Gillespie–Nyholm aspects of the force fields. I. Points-on-a-sphere and Extended Hückel Molecular orbital analyses of trigonal bipyramids. Journal of the American Chemical Society, 95, 3097–3104.

Bartell, L. S. (1984) 'Do the VSEPR points-on-a-sphere repulsions simulate quantum interactions?' Croatia Chimica Acta, in press.

Baur, W. H. (1970) Bond length variation and distorted coordination polyhedra in inorganic crystals. Transactions of the American Crystallographic Association 6, 129–155.

Baur, W. H. (1981a) Interatomic distance predictions for computer simulation of crystal structures. In M. O'Keeffe and A. Navrotsky, Eds., Structure and Bonding in Crystals, vol. II, p. 31–52. Academic Press, New York.

Baur, W. H. (1981b) Three dimensionally periodic, eleven coordinated, dense packing of symmetry equivalent spheres. Material Research Bulletin, 16, 339–345.

Baur, W. H. and McLarnan, T. J. (1982) Observed wurtzite derivatives and related dipolar tetrahedral structures. Journal of Solid State Chemistry, 42, 300–321.

Baur, W. H., Tillmanns, E., and Hofmeister, W. (1983) Topological analysis of crystal structures. Acta Crystallographica, B44, 669–673.

Bragg, W. H. (1930) The structures of silicates. Zeitschrift für Kristallographie, 74, 237–305.

Burdett, J. K. (1976) The shapes of main group molecules: A simple semiquantitative molecular orbital approach. Structure and Bonding, 31, 67–105.

Burdett, J. K. (1979) Structural correlations in small molecules: A simple molecular orbital treatment of sp mixing. Inorganic Chemistry, 18, 1024–1030.

Burdett, J. K. (1980) Molecular Shapes. Wiley-Interscience, New York.

Burdett, J. K., Price, G. D., and Price S. L. (1981) The factors influencing solid state structure. An interpretation using pseudopotential radii structure maps. Physical Review, B24, 2903–2912.

Burdett J. K. (1982) The prediction of the structures of complex solids. Advances in Chemical Physics, 49, 47–113.

Burdett, J. K., Haaland, P., and McLarnan, T. J. (1981) A study of the arsenic, black phosphorus and other structures derived from rocksalt by bondbreaking processes: II. Band structure calculations and the importance of the gauche effect. Journal of Chemical Physics, 75, 5774–5781.

Burdett, J. K. and McLarnan, T. J. (1982) An orbital explanation for Pauling's third rule. Journal of the American Chemical Society, 104, 5229–5230.

Burdett, J. K., Price, G. D., and Price, S. L. (1982) Role of the Crystal Field Theory in determining the structures of spinels. Journal of the American Chemical Society, 104, 92–95.

Bloch, A. N. and Schatteman, G. C. (1981) Quantum defect orbital radii. In M. O'Keeffe and A. Navrotsky Eds., Structure and Bonding in Crystals vol. I. p. 49–72. Academic Press, New York.

Caro, P. E. (1968) OM_4 tetrahedra linkages and the cationic group $(MO)_n^{n+}$ in rare earth oxides and oxysalts. Journal of Less-Common Metals, 16, 367–377.

Caro, P. E. (1972) Anion centered coordination polyhedra and related physical properties in rare earth oxides and oxysalts. In NBS Special Publication 364, Solid State Chemistry, Proceedings of 5th Materials Reserach Symposium.

Chadi, D. J. and Cohen, M. L. (1973) Special points in the Brillouin zone. Physical Review, B8, 5747–5753.

Chen, M. M. L. and Hoffmann, R. (1976) Sulfuranes. Theoretical Aspects of Bonding, Substituent Site Preferences and Geometrical Distortions. Journal of the American Chemical Society, 98, 1647–1653.

Dill, J. D., von R. Schleyer, P., Binkley J. S., and Pople, J. A. (1977) Molecular Orbital Theory of the Electronic Structures of Molecules, 34. Structures and Energies of Small Compounds Containing Lithium or Beryllium. Ionic, Multicenter and Coordinate Bonding. Journal of the American Chemical Society, 99, 6159–6173.

Franzen, H. F. (1966) On the bonding of S, Se and Te in transition metal monochalcogenides. Journal of Inorganic and Nuclear Chemistry, 28, 1575–1579.

Gibbs, G. V., Meagher, E. P., Newton, M. D., and Swanson, D. K. (1981) A comparison of experimental and theoretical bond length and angle variations for minerals, inorganic solids and molecules. In M. O'Keeffe and A. Navrotsky, Eds., Structure and Bonding in Crystals, vol. I, p. 195–226. Academic Press, New York.

Gillespie, R. J. (1972) Molecular Geometry. Van Nostrand-Rheinhold, London.

Hoffman, R. (1962) An Extended Hückel Theory. I. Hydrocarbons. Journal of Chemical Physics, 39, 1397–1412.

Hoffman, R. (1971) Interaction of orbitals through space and through bonds. Accounts of Chemical Research, 4, 1–9.

Hoffman, R. and Lipscomb, W. N. (1962) Theory of polyhedral molecules. I. Physical factorizations of the secular equation. II. A crystal field model. Journal of Chemical Physics, 36, 2179–2195.

Howie, R. A. and West, A. R. (1974) The crystal structure of high (γ)-Li_2 $BeSiO_4$: a tetrahedral structure. Acta Crystallographica, B30, 2434–2437.

Laurent, Y., Gerkov, F. F., David, J., and Guyader, J. (1980) LiSiON: Etude d'une structure tetraedrique de type wurtzite presentant un nouvel arrangement atomique. Annales de Chimie Français 5, 647–655.

Laurent, Y., Guyader, J., and Roult, G. (1981) Etude par diffraction de neutrons selon la methode du temps de vol de LiSiON. Acta Crystallographica, B37, 911–913.

Marezio, M. (1965) The crystal structure and anomalous dispersion of γ-$LiAlO_2$. Acta Crystallographica, 19, 396–400.

McLarnan, T. J. and Baur, W. H. (1982) Enumeration of wurtzite derivatives and related dipolar tetrahedral structures. Journal of Solid State Chemistry, 42, 283–299.

McLarnan, T. J., Hill, D. J., and Gibbs, G. V. (1979) A CNDO/2 molecular orbital study of shared tetrahedral edge conformations in olivine-type compounds. Australian Journal of Chemistry, 32, 949–959.

Moore, P. B. and Araki, T. (1978) Dumortierite, $Si_3B[Al_{6.75}\square_{0.25}O_{17.25}(OH)_{0.75}]$: a detailed structure analysis. Neues Jahrbuch für Mineralogie Abhandlungen, 132, 231–241.

Newton, M. D. (1981) Theoretical probes of bonding in the disiloxy group. In M. O'Keeffe and A. Navrotsky, Eds., Structure and Bonding in Crystals, vol. I, p. 175–193. Academic Press, New York.

O'Keeffe, M. and Hyde, B. G. (1978) Non-bonded interactions and the crystal chemistry of tetrahedral structures related to the wurtzite type (B4). Acta Crystallographica, B34, 3419–3528.

O'Keeffe, M. and Hyde, B. G. (1981) The role of nonbonded forces in crystals. In M. O'Keeffee and A. Navrotsky, Eds., Structure and Bonding in Crystals, vol. I, p. 227–254. Academic Press, New York.

O'Keeffe, M. and Hyde, B. G. (1982) Anion Coordination and cation packing in oxides. Journal of Solid State Chemistry, 44, 24–31.

O'Keeffe, M., Shavers, C. L., and Hyde, B. G. (1981) Cation packing and molar volume in oxides and nitrides with the wurtzite structure. Journal of Solid State Chemistry, 39, 265–267.

Pauling, L. (1929) The principles determining the structure of complex ionic crystals. Journal of the American Chemical Society, 51, 1010–1026.

Pauling, L. (1960) The Nature of the Chemical Bond, 3rd ed. Cornell Univ. Press, Ithaca, New York.

Pearson, R. G. (1966) Acids and bases. Science, 151, 172–177.

Ramberg, H. (1952) The Origin of Metamorphic and Metasomatic Rock. The University of Chicago Press, Chicago.

Shaffer, P. T. B. (1969) A review of the structure of silicon carbide. Acta Crystallographica, B25, 477–481.

Shannon, R. D. (1976) Revised effective ionic radii and systematic studies of interatomic distances in halides and chalcogenides. Acta Crystallographica, A32, 751–767.

Smith, D. K., Cline, C. F., and Austerman, S. B. (1965) The crystal structure of β-beryllia. Acta Crystallographica, 18, 393–397.

St. John, J. and Bloch, A. N. (1974) Quantum-defect electronegativity scale for non-transition elements. Physical Review Letters, 33, 1095–1098.

Tossell, J. A. and Gibbs, G. V. (1978) The use of molecular orbital calculations on model systems for the prediction of bridging-bond-angle variations in siloxanes, silicates, silicon nitrides and silicon sulfides. Acta Crystallographica, A34, 463–472.

Wells, A. F. (1975) Structural Inorganic Chemmistry. Oxford University Press, New York.

Whangbo M-H, Hoffmann, R., and Woodward, R. B. (1978) Conjugated one and two dimensional polymers. Proceedings of The Royal Society of London, A366, 23–46.

Zunger, A. and Cohen, M. L. (1978) Density-functional pseudopotential approach to crystal phase stability and electronic structure. Physical Review Letters, 41, 53–56.

Manuscript received, February 15, 1983;
accepted for publication, March 15, 1984.

Appendix 1: Geometrical and Atomic Parameters

Our calculations were of the extended Hückel type (Hoffman, 1962; Hoffmann and Lipscomb, 1962) and employed, for the crystalline materials the standard tight-binding approach (from Whangbo et al., 1978, for example). The band structure program was written by M-H Whangbo (North Carolina State University). Calculations on crystalline BeO used Slater exponents 0.975 (Be) and 2.275 (O). The H_{ii} (in eV) were -10.0 (Be2*s*), -6.0 (Be2*p*), -32.3 (O2*s*) and -14.8 (O2*p*). The Be–O bond distance was 1.649Å. The wurtzite type and other close-packed structures had the anions in an ideal h.c.p. arrangement. In β-BeO the angle O–Be–O between the two Be–O bonds in a four-membered ring was varied, keeping d(Be–O) = 1.649Å. The O–Be–O angle between the two "back" bonds not in the 4-ring was set equal to 109.47°. Calculations on OBe_4 "molecules" used the same bond distance and oxygen parameters, but allowed only 2*s* orbitals on Be with $H_{ii} = -8.0$ eV.

Calculations on MgAlON used the above oxygen parameters. Other Slater exponents were 1.950 (N) and 1.058 (Mg and Al). Coulomb integrals were -26.0 (N2*s*), -13.4 (N2*p*), -9.0 (Mg3*s*), -4.5 (Mg3*p*), -12.3 (Al3*s*) and -6.5 (Al3*p*). In some calculations O and N were replaced with an averaged anion whose Slater exponent and H_{ii} were the arithmetic means of those for O and N. The crystal structures used were ideal h.c.p. arrangements with a volume per anion equal to that reported for MgAlON by O'Keeffe et al. (1981).

Calculations on SiO_2 in the rutile and α-PbO_2 types used the O parameters above. The Slater exponent for Si was 1.383 and its H_{ii} were -17.3 (3*s*) and -9.2 (3*p*). No *d* orbitals were included. The crystal structures were idealized to hexagonal close-packings with a Si–O distance for 6-coordinate silicon of 1.77Å. The calculations on one-dimensional chains replaced the terminal Si by Si' having only a 3*s* orbital at -13.2 eV.

The H_{ij} were computed by using the arithmetic mean Wolfsberg–Helmholz formula with K = 1.75. Energies were computed using the special points method (Baldareschi, 1973; Chadi and Cohen, 1973). Here is not the place to discuss the details of the tight-binding approach we have used. The enquiring reader should refer to Whangbo et al. (1978) for a discussion.

Appendix 2: Perturbation Theoretic Results

For two orbitals φ_1 and φ_2 with energies $H_{11} < H_{22} < 0$, the Extended Hückel secular determinant is

$$0 = \det \begin{vmatrix} H_{11} - E & H_{12} - S_{12}E \\ H_{21} - S_{21}E & H_{22} - E \end{vmatrix}$$

If we assume $H_{ij} = \frac{K}{2} S_{ij} (H_{ii} + H_{jj})$ with K = 2, and write $E = H_{11} + \epsilon$ this becomes

$$0 = \det \begin{vmatrix} -\epsilon & (H_{22} - \epsilon)S_{12} \\ (H_{22} - \epsilon)S_{12} & H_{22} - H_{11} - \epsilon \end{vmatrix}$$

$$= -\epsilon(H_{22} - H_{11} - \epsilon) - (H_{22} - \epsilon)^2 S_{12}^2 \qquad (1)$$

If we are interested only in the stabilization of the lower energy orbital, φ_1 we may assume ϵ is small. Explicitly, we assume H_{22} and $H_{22} - H_{11}$ are of the same order and that ϵ and $S_{12}^2 H_{22}$ are of the same order and are small compared to H_{22}. Equation (1) can then be written to first order in ϵ as

$$-\epsilon_0 (H_{22} - H_{11}) - H_{22}^2 S_{12}^2 = 0, \text{ i.e., } \epsilon_0 = -\frac{H_{22}^2 S_{12}^2}{H_{22} - H_{11}}.$$

Since ϵ_0 is of order $(H_{22}S_{12})^2$, this is called the second order correction to the energy. To find the fourth order correction to the energy, we let $\epsilon = \epsilon_0 + \eta$ in (1). Now all terms linear in ϵ_0 or quadratic in S_{12} cancel, and the largest remaining terms are those involving η, ϵ_0^2 or S_{12}^4. Keeping these terms only in (1) gives $-\eta_0(H_{22} - H_{11}) + \epsilon_0^2 + 2H_{22}\,\epsilon_0 S_{12}^2 = 0$, so that

$$\eta_0 = \frac{\epsilon_0^2}{H_{22} - H_{11}} + \frac{2H_{22}\epsilon_0 S_{12}^2}{H_{22} - H_{11}} = \frac{H_{22}^4 S_{12}^4}{(H_{22} - H_{11})^3} - \frac{2H_{22}^3 S_{12}^4}{(H_{22} - H_{11})^2}$$

To find the wavefunction ψ of the lower energy molecular orbital to second order, write $\psi = c_1\varphi_1 + c_2\varphi_2$ and solve simultaneously the secular equations

$$(H_{11} - E)c_1 + (H_{12} - S_{12}E)c_2 = 0$$

$$(H_{12} - S_{12}E)c_1 + (H_{22} - E)c_2 = 0$$

Using

$$E = H_{11} + \epsilon_0 = H_{11} - \frac{H_{22}^2 S_{12}^2}{H_{22} - H_{11}}$$

and ignoring terms smaller than second order yields

$$c_2 = \frac{H_{22}S_{12}}{H_{11} - H_{22}} c_1 ,$$

so that when properly normalized,

$$\psi = \left(1 - \frac{(2H_{11}H_{22} - H_{22}^2)S_{12}^2}{2(H_{22} - H_{11})^2}\right)\varphi_1 - \frac{H_{22}S_{12}}{H_{22} - H_{11}}\varphi_2$$

Higher order wavefunctions are found in the same way.

Between typical pairs of real atoms, S_{12}^2 is not independent of $H_{22} - H_{11}$, but is roughly proportional to $(H_{22} - H_{11})^{-1}$. In the calculations below, we assume $S_{12}^2 \alpha (H_{22} - H_{11})^{-n}$, $n \geq 0$, which includes both this case and the case S_{12} = constant (as in some of the numerical computations discussed in the text).

Now let φ_1, φ_2, φ_3 and φ_4 be four atomic orbitals with $H_{11} < H_{22} < H_{33} < H_{44} < 0$. Orbitals φ_1 and φ_2 are to lie on anions, φ_3 and φ_4 on cations. For convenience, we denote H_{ii} simply by H_i. In all our calculations the occupied orbitals are strongly anion-located, so it is enough to look at how various interactions perturb orbitals φ_1 and φ_2. We now prove remarks 1–4 from the text.

Remark 1: A crystal containing interactions (φ_1, φ_4) and (φ_2, φ_3) is more stable than one containing interactions (φ_1, φ_3) and (φ_2, φ_4).

Proof: The second order stabilization resulting from the first pair of interactions is $-(H_4^2S_{14}^2)/(H_4 - H_1) - (H_3^2S_{23}^2)/(H_3 - H_2)$, and the stabilization resulting from the second pair is $-(H_3^2S_{13}^2)/(H_3 - H_1) - (H_4^2S_{24}^2)/(H_4 - H_2)$. If $S_{ij}^2 \alpha (H_j - H_i)^{-n}$, then the difference between these two stabilizations is proportional to

$$-\frac{H_4^2}{(H_4 - H_1)^{n+1}} - \frac{H_3^2}{(H_3 - H_2)^{n+1}} + \frac{H_4^2}{(H_4 - H_2)^{n+1}} + \frac{H_3^2}{(H_3 - H_1)^{n+1}} .$$

This can be written as $f(H_2) - f(H_1)$,

$$\text{where } f(x) = \frac{H_4^2}{(H_4 - x)^{n+1}} - \frac{H_3^2}{(H_3 - x)^{n+1}} .$$

We would like to show $f(H_2) - f(H_1) < 0$, for which it is enough to show that $\frac{df}{dx} < 0$ for $x < H_3$. A bit of algebra yields

$$\frac{df}{dx} = (n + 1)\{H_4^2(H_3 - x)^{n+2} - H_3^2(H_4 - x)^{n+2}\}/(H_3 - x)^{n+2}(H_4 - x)^{n+2}$$

The denominator of this expression is positive whenever $x < H_3$. Further, $H_3^2 > H_4^2$ and $H_4 - x > H_3 - x > 0$, so the numerator is negative, as desired.

Remark 2: If the pair of interactions (φ_1, φ_3), (φ_2, φ_4) is replaced by (φ_1, φ_4), (φ_2, φ_3), charge migrates away from orbitals φ_2 and φ_4 and toward orbitals φ_1 and φ_3.

Proof: It is obvious that since the energy decreases in this process, there must be some such movement of charge from higher to lower energy orbitals. To work out the details, we construct the wavefunctions to second order. In the first case, the two occupied molecular orbitals will be

$$\left(1 - \frac{(2H_1H_3 - H_3^2)S_{13}^2}{2(H_3 - H_1)^2}\right)\varphi_1 - \frac{H_3S_{13}}{H_3 - H_1}\varphi_3$$

and

$$\left(1 - \frac{(2H_2H_4 - H_4^2)S_{24}^2}{2(H_4 - H_2)^2}\right)\varphi_2 - \frac{H_4S_{24}}{H_4 - H_2}\varphi_4 .$$

In the second case, the orbitals will have the same form but with subscripts (1,4) and (2,3). To compute the orbital charges resulting from a normalized orbital $a\varphi_i + b\varphi_j$, one observes that the charge density is $a^2\varphi_i^2 + 2ab\varphi_i\varphi_j + b^2\varphi_j^2$. If the charge coming from φ_i^2 is assigned to orbital φ_i the charge coming from φ_j^2 is assigned to φ_j, and the bond density from φ_i φ_j is divided evenly, and if the orbital contains two electrons, then the number of electrons in φ_i is $2a^2 + 2abS_{ij}$, and the number of electrons in φ_j is $2b^2 + 2abS_{ij}$. Applying this formula to the orbitals above and ignoring terms of degree greater than 2 in S_{ij} results in the atomic orbital occupancies shown in Table 8. The inequalities listed in that Table are those we prove here.

If $S_{ij}^2 \alpha (H_j - H_i)^{-n}$, then to prove the relationship claimed for the charges on orbital 3 amounts to showing that

$$\frac{H_1H_3}{(H_3 - H_1)^{n+2}} < \frac{H_2H_3}{(H_3 - H_2)^{n+2}} ,$$

i.e., that

$$\frac{H_1}{(H_3 - H_1)^{n+2}} > \frac{H_2}{(H_3 - H_2)^{n+2}} .$$

Table 8. Charges from perturbation theory

Interactions	(1,3);(2,4)		(1,4);(2,3)
Orbital	Charge		
1	$2-2\left\{\frac{H_1H_3S_{13}^2}{(H_3-H_1)^2}\right\}$	<	$2-2\left\{\frac{H_1H_4S_{14}^2}{(H_4-H_1)^2}\right\}$
2	$2-2\left\{\frac{H_2H_4S_{24}^2}{(H_4-H_2)^2}\right\}$	>	$2-2\left\{\frac{H_2H_3S_{23}^2}{(H_3-H_2)^2}\right\}$
3	$2 \cdot \frac{H_1H_3S_{13}^2}{(H_3-H_1)^2}$	<	$2 \cdot \frac{H_2H_3S_{23}^2}{(H_3-H_2)^2}$
4	$2 \cdot \frac{H_2H_4S_{24}^2}{(H_4-H_2)^2}$	>	$2 \cdot \frac{H_1H_4S_{14}^2}{(H_4-H_1)^2}$

[a] The charges on four atomic orbitals in the case that interactions exist between orbitals 1 and 3 and between 2 and 4 (left column) and in the case that the interacting pairs are (1,4);(2,3) (right column).

It therefore suffices to show that

$$\frac{d}{dx}\left(\frac{x}{(H_3 - x)^{n+2}}\right) < 0$$

when $x < H_3$. This derivative is $(H_3 + (n + 1)x)/(H_3 - x)^{n+3}$. Since $x < H_3 < 0$, this is negative, as desired. The proofs for the other three orbitals are identical.

Remark 3: Increasing p_{anion} decreases the bond overlap population between the anion and a given metal neighbor.

Proof: We show that if $H_1 < H_2$, $H_1 < H_3$, φ_1 interacts with φ_2 and φ_3 and $S_{23} = 0$ then the bond overlap population between orbitals 1 and 2 increases as H_3 increases. We first treat this three orbital problem just as we did the two orbital problem above, and find that the lowest energy molecular orbital has, to fourth order, a normalized wavefunction of the form

$$\left(1 - \frac{(2H_1H_2 - H_2^2)S_{12}^2}{2(H_2 - H_1)^2} - \frac{(2H_1H_3 - H_3^2)S_{13}^2}{2(H_3 - H_1)^2} + O(S^4)\right)\varphi_1$$

$$+ \left(-\frac{H_2S_{12}}{H_2 - H_1} + \frac{4(H_1H_2^2 - H_2^3)S_{12}^3}{2(H_2 - H_1)^3} + \frac{S_{12}S_{13}^2}{(H_2 - H_1)(H_3 - H_1)}\right.$$

$$\left.\left[\frac{H_1H_3^2}{H_2 - H_1} + \frac{H_2(2H_1H_3 - H_3^2)}{2(H_3 - H_1)}\right] + O(S^5)\right)\varphi_2$$

$$+ \left(-\frac{H_3S_{13}}{H_3 - H_1} + \frac{(4H_1H_3^2 - H_3^3)S_{13}^3}{2(H_3 - H_1)^3} + \frac{S_{13}S_{12}^2}{(H_3 - H_1)(H_2 - H_1)}\right.$$

$$\left.\left[\frac{H_1H_2^2}{H_3 - H_1} + \frac{H_3(2H_1H_2 - H_2^2)}{2(H_2 - H_1)}\right] + O(S^5)\right)\varphi_3$$

In this wavefunction, we may assume S_{12} and S_{13} are positive (otherwise just replace φ_2 or φ_3 by $-\varphi_2$ or $-\varphi_3$).

In a normalized molecular orbital $c_1\varphi_1 + c_2\varphi_2 + c_3\varphi_3$ the bond overlap population between atomic orbitals 1 and 2 is $4c_1c_2S_{12}$. For this wavefunction that population is

$$4S_{12}\left(-\frac{H_2S_{12}}{H_2 - H_1} + \frac{(3H_1H_2^2 - H_2^3)S_{12}^3}{(H_2 - H_1)^3} + \frac{H_1H_3^2S_{12}S_{13}^2}{(H_2 - H_1)^2(H_3 - H_1)}\right.$$

$$\left. + \frac{H_2(2H_1H_3 - H_3^2)S_{12}S_{13}^2}{(H_2 - H_1)(H_3 - H_1)^2} + O(S^5)\right)$$

Only the third and fourth of these terms involve H_3, so to show that the bond overlap population increases as H_3 increases, it suffices to prove the derivatives of these two terms with respect to H_3 are positive whenever $H_1 < H_3 < 0$. Assuming that $S_{13}^2 \alpha (H_3 - H_1)^{-n}$, the derivative of the the third term is proportional to

$$\frac{4\,H_1H_3S_{12}^2}{(H_2 - H_1)^2(H_3 - H_1)^{n+2}}\{2(H_3 - H_1) - (n + 1)H_3\}.$$

Since the quantity in braces is positive and H_1H_3 is positive, this is greater than 0. By a similar argument, the derivative of the fourth term is also positive, as desired.

Remark 4: Anions of the same species prefer to occupy sites of equal bond strength sum. This preference is not due to energy differences of order S^2 like those in Remark 1, but to (smaller) energy differences of order S^4.

Proof: Let $H_1 < H_2 < H_3 < 0$. We shall show that the energy of a pair of orbitals φ_1, one of them interacting with two φ_2 orbitals and one with two φ_3 orbitals, is greater than that of a pair of φ_1 orbitals, each interacting with one φ_2 and one φ_3. The difference between these energies appears only in fourth order S_{ij}.

The second order energetic stabilization resulting from interacting φ_1 with φ_2 and φ_3 (i.e., forming a "molecule" $\varphi_1\varphi_2\varphi_3$) is

$$-\frac{H_3^2S_{13}^2}{H_3 - H_1} - \frac{H_2^2S_{12}^2}{H_2 - H_1}$$

Similarly, a "molecule" $\varphi_1\varphi_2\varphi_2$ is stabilized by

$$-2\frac{H_2^2S_{12}^2}{H_2 - H_1},$$

and $\varphi_1\varphi_3\varphi_3$ is stabilized by

$$-2\frac{H_3^2S_{13}^2}{H_3 - H_1}.$$

Hence, to second order, two $\varphi_1\varphi_2\varphi_3$ "molecules are stabilized by exactly as much as one $\varphi_1\varphi_2\varphi_2$ and one $\varphi_1\varphi_3\varphi_3$ "molecule."

Define ϵ_2 to be

$$-\frac{H_2^2S_{12}^2}{H_2 - H_1}$$

and ϵ_3 to be

$$-\frac{H_3^2S_{13}^2}{H_3 - H_1}.$$

Then the fourth order contribution to the energy of $\varphi_1\varphi_2\varphi_3$ is

$$\left(\frac{1}{(H_2 - H_1)} + \frac{1}{(H_3 - H_1)}\right)(\epsilon_2 + \epsilon_3)^2 + \frac{\epsilon_2 + \epsilon_3}{(H_2 - H_1)(H_3 - H_1)}\cdot$$

$$\{H_2^2S_{12}^2 + H_3^2S_{13}^2 + 2H_2(H_3 - H_1)S_{12}^2 + 2H_3(H_2 - H_1)S_{13}^2\} =$$

$$\left(\frac{1}{H_2 - H_1} + \frac{1}{H_3 - H_1}\right)(\epsilon_2 + \epsilon_3)^2$$

$$+ (\epsilon_2 + \epsilon_3)\left\{-\frac{\epsilon_2}{H_3 - H_1} - \frac{\epsilon_3}{H_2 - H_1} + \frac{2H_2S_{12}^2}{H_2 - H_1} + \frac{2H_3S_{13}^2}{H_3 - H_1}\right\}$$

$= \epsilon_2^2\beta_2 + \epsilon_2\epsilon_3(\beta_2 + \beta_3) + \epsilon_3^2\beta_3 + (\epsilon_2 + \epsilon_3)(\gamma_2 + \gamma_3)$, where

$$\beta_i = \frac{1}{H_i - H_1}$$

and

$$\gamma_i = \frac{2H_iS_{1i}^2}{H_i - H_1}.$$

Obviously, then, the fourth order contribution to the energy of the bonding orbital of $\varphi_1\varphi_2\varphi_2$ is $4\varepsilon_2^2\beta_2 + 4\varepsilon_2\gamma_2$, and the fourth order contribution to $\varphi_1\varphi_3\varphi_3$ is $4\varepsilon_3^2\beta_3 + 4\varepsilon_3\gamma_3$. The difference in energy between $2(\varphi_1\varphi_2\varphi_3)$ and $(\varphi_1\varphi_2\varphi_2 + \varphi_1\varphi_3\varphi_3)$ (each molecule having 2 electrons in the lowest energy orbital) is then $4(\varepsilon_2 - \varepsilon_3)$

$(\beta_3\epsilon_3 - \beta_2\epsilon_2) + 4(\epsilon_2 - \epsilon_3)(\gamma_3 - \gamma_2)$. We would like to show that this is negative, which follows at once from the obvious inequalities $\epsilon_2 < \epsilon_3 < 0$, $\gamma_2 < \gamma_3 < 0$, and $0 < \beta_3 < \beta_2$. This completes the proof of remark 4.

It is worth remarking that in special cases like S_{ij} = constant or $n = 1$ all of the proofs above simplify to yield arguments more like that given in the body of the paper for Remark 1. We have attempted here to present proofs as general as possible in order both to suggest the range of validity of our results and to show that such simplifying assumptions are unnecessary.